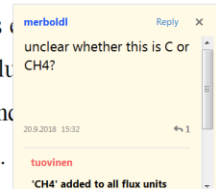


This document consists of the following parts: (1) Reply to the comments presented by the Associate Editor; (2) Overview of the changes to each section of the manuscript; (3) Summary of the revisions in response to reviewers' comments. For further discussion of the comments, please see our original replies (<https://doi.org/10.5194/bg-2018-155-AC1> and <https://doi.org/10.5194/bg-2018-155-AC2>); (4) Marked-up manuscript indicating the changes. In addition to the revisions reported in (2) and (3), there are linguistic and stylistic corrections throughout the manuscript.

(1) REPLY TO ASSOCIATE EDITOR

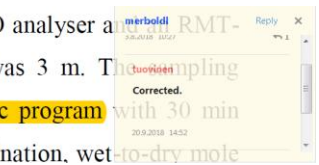
10

location bias. We found that methane (CH₄) fluxes varied strongly with wind direction (from -0.09 to $0.59 \mu\text{g m}^{-2} \text{s}^{-1}$ on average), reflecting the distribution of different LCCs. Using footprint weights of grouped LCCs as a function of wind direction for the measured CH₄ flux, we then developed a multiple regression model to estimate LCC-specific fluxes. We found that wet fen and graminoid tundra patches in locations with a high topography-based wetness index were significant sources ($0.95 \mu\text{g m}^{-2} \text{s}^{-1}$), while mineral soils were significant sinks ($-0.13 \mu\text{g m}^{-2} \text{s}^{-1}$).



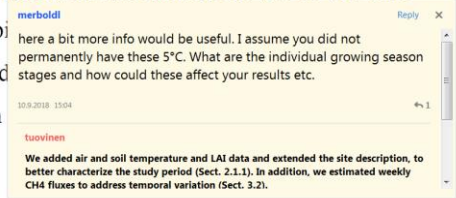
merboldi
unclear whether this is C or CH4?
20.9.2018 15:32
tuovinen
'CH4' added to all flux units

Germany) sonic anemometer/thermometer, an LI-7000 (LI-COR, Inc., Lincoln, NE, USA) CO₂/H₂O analyser and a LI-8000 (LI-COR, Inc., Lincoln, NE, USA) CH₄ analyser. The measurement height was 3 m. The sampling frequency was 10 Hz, and the turbulent fluxes were calculated with the in-house **PyBARFlucCalc** program. The fluxes were calculated using block averaging according to standard procedures, including double coordinate rotation, lag determination, wet-to-dry mole fraction conversion and high-frequency flux loss correction where necessary (Aubrey et al., 2014). The data were screened for instationarity, weak turbulence (friction velocity $< 0.12 \text{ m s}^{-1}$) and low wind speed ($< 1 \text{ m s}^{-1}$). The data analysed in the present study cover the period of 5 July to 29 August 2014, which was a warm year, using the daily mean air temperature of $5 \text{ }^\circ\text{C}$ as the threshold.

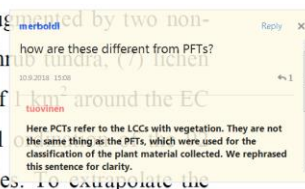


merboldi
RMT-200 sampling frequency with 30 min
Corrected.
20.9.2018 14:32
tuovinen

The land cover classification was based on seven visually judged **plant community types (PCTs)** augmented by two non-vegetated surfaces: (1) **wet fen**, (2) **dry fen**, (3) **bog**, (4) graminoid tundra, (5) flood meadow, (6) shrub tundra, (7) heath tundra, (8) bare ground and (9) water (Mikola et al., 2018). The PCTs were identified within an area of 1 km^2 around the EC tower on the basis of an extensive vegetation and soil survey. They were verified using statistical analysis of the established study plots according to plant species composition and functional plant and soil attributes. To extrapolate the



merboldi
here a bit more info would be useful. I assume you did not permanently have these 5°C. What are the individual growing season stages and how could these affect your results etc.
10.9.2018 15:04
tuovinen
We added air and soil temperature and LAI data and extended the site description, to better characterize the study period (Sect. 2.1.1). In addition, we estimated weekly CH4 fluxes to address temporal variation (Sect. 3.2).



merboldi
how are these different from PFTs?
20.9.2018 15:09
tuovinen
Here PCTs refer to the LCCs with vegetation. They are not the same thing as the PFTs, which were used for the classification of the plant material collected. We rephrased this sentence for clarity.

The land cover classification was based on seven visually judged **plant community types (PCTs)** augmented by two non-vegetated surfaces: (1) **wet fen, (2) dry fen, (3) bog,** (4) graminoid tundra, (5) flood tundra, (8) bare ground and (9) water (Mikola et al., 2018). The PCTs were identified tower on the basis of an extensive vegetation and soil survey. They were verified established study plots according to plant species composition and functional plant

merboldl
how can one distinguish between wet and dry fen only visually?
3.8.2018 10:21
tuovinen
We included a more detailed description of the LCC characteristics, which indicates the difference between the fen types (Table 2).

1b). **The internal and external classification accuracy of the land cover classification were 80 and 49 %, respectively. For details, see Mikola et al. (2018).**

Using non-linear regression, the LAI of vascular plants was estimated (NDVI) calculated from the reflectance data of the 2012 WorldView-2

merboldl
why one approach 80% and one only 49% . please expand here
3.8.2018 10:31
tuovinen
Definitions of 'internal' and 'external' were included.

To demonstrate how the EC flux measurement at Tiksi is affected by surface heterogeneity, we calculated with Eq. (8) the footprint-weighted averages of **the surface attributes LAI, terrain elevation and TWI,** and with Eq. (10) the footprint-weighted LCC areas of the nine classes shown in Fig. 1a. I the variables that affect the footprint in a given θ , i.e., U , conditions, for which typical parameter combinations were

merboldl
you mention above that LAI and terrain elevation are continuous variables - can you extend on this please
3.8.2018 10:40
tuovinen
This simply means that LAI, elevation and TWI are expressed as real (decimal) numbers, while land cover is expressed as a class (an integer or a name). We rephrased the sentence for clarity.

for a representative site description. **Even if the coverage of the nine basic LCCs clearly differs from their footprint-weighted contributions (Table 4), the four classes aggregated according to their assumed CH₄ emission potential cover areas rather similar to those within the original study domain (Table 6).** Within the regional upscaling area of 35.8 km², the strong emitters are less common, but the total flux is only freshwater bodies occupy a larger relative area (Table

merboldl
introducing nine classes in the begining but then in any case only using realistically 4 is rather misleading and this needs to be adresses in the revised manuscript
10.9.2018 15:29
tuovinen
We start from the general land cover classification (which is also used in other studies), which we apply in the present M5 to analyse CH4 fluxes. For this, four aggregated classes was an appropriate choice, as it represents the different levels of CH4 exchange expected on different land cover types. To clarify, we reformulated this paragraph and, in a new section that addresses modelling uncertainties, explain that the uncertainties preclude modelling that could resolve all individual LCCs. We also replaced 'LCC-specific' by 'LCC group-specific' throughout the text, where appropriate.

5

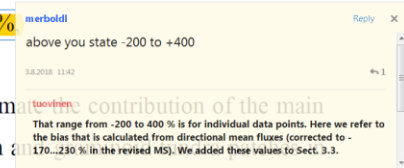
The eddy covariance flux measurement technique is commonly considered to have an advantageous spatial averaging property, sometimes to the extent that it is assumed to "provide an accurate integration of the overall flux from the [heterogeneous] ecosystem" (Turner and Chapin III, 2006). However,

universal premise, since this integration process involves different feature of EC measurements, which we in the present study demonstrate in northeastern Russia. The CH₄ fluxes measured at Tiksi were high and soil wetness within the tundra landscape around the EC tower.

merboldl
I suggest to read Hill et al. 2016 with Robert Clement on what an EC System sees and what it can not see.
3.8.2018 11:42
tuovinen
This is a very useful paper; thank you for pointing it out. We cite it in the revised MS in a few places, but not here. The highlighted sentence refers to the variation within the footprint, i.e. the representativeness problem, while Hill et al. address the region outside the footprint, i.e. the fluxes we do not measure (ecosystem averaging/upscaling problem). These are separate issues.

and soil wetness within the tundra landscape around the EC tower. During summer 2014, the mean bias of observations with respect to the upscaled flux varied strongly with wind direction, ranging from **-200 to 200 %**

By combining VHSR satellite imagery and footprint modelling, we could statistically estimate the contribution of the main land cover types to EC measurements. Methane emissions mainly originated from wet fen and



5 (2) OVERVIEW OF CHANGES

Abstract

- updated to reflect the revisions to the main text
- language improved

10 **Introduction**

- presentation improved by removing secondary material
- scope of the manuscript highlighted

Material and methods

Section 2.1.1

- 15 - site description enhanced
- meteorological data for 2014 added, including a new figure (Fig. S1)

Section 2.1.2

- description of EC data processing methods extended
- description of chamber measurements included

20 **Section 2.1.3**

- table summarizing LCC characteristics added (Table 1)
- LAI dynamics and LCC validation clarified

Section 2.1.4

- LCC description extended
- 25 - LAI data included

Section 2.2.1

- removed

Section 2.2.2 (now 2.2.1)

- updated to match the removal of Sect. 2.2.1

Sections 2.2.3–4 (now 2.2.2–3)

- minor changes only

5 **Section 2.3.1**

- some methodological details clarified to coordinate with Sect. 2.3.2
- measurement error estimation and weekly data analysis added

Section 2.3.2

- some methodological details clarified

10 **Results and discussion**

Section 3.1

- shortened considerably
- number of upscaling reference scales reduced, Table 4 simplified
- presentation improved; a minor result updated

15 **Section 3.2**

- new results based on weekly data added, including a new figure (Fig. 6)
- new results on environmental controls added
- a substantial amount of new discussion and references added
- literature-based flux data corrected as a result of more thorough analysis

- 20 - a paragraph moved to a new section (Sect. 3.4)

Section 3.3

- discussion of upscaling reference scales simplified, Table 6 reduced
- flux sensor bias estimates corrected and enhanced
- measurement uncertainty included

25 **Section 3.4**

- new section on methodological issues
- previous paragraph on LCC accuracy and some text from the Conclusions adapted
- new material on footprint uncertainty, including a summary of validation studies
- new discussion on the feasibility and limitations of the statistical model employed

30

Conclusions

- *shortened for enhanced focus on key results and implications*
- *presentation improved and results updated*

References

- 5 - *list updated according to the text changes*

Tables

- *one table added (new Table 1)*
- *one table moved to the Supplement (old Table 3)*
- *two tables modified substantially (Tables 4 and 6)*

10 **Figures**

- *Fig. 1: labels (a)–(d) added*
- *Fig. 1a: readability improved by changing the LCC colour codes*
- *Fig 4a–c: new right axes introduced*
- *Fig. 4d–f: removed*

- 15 - *Fig. 6: new material*
- *Fig. 7 (old Fig. 6): confidence interval included, appearance updated*

Supplement

- *footprint analysis added, based on previous Sects. 2.2.1 and 3.1*
 - *Fig. S1: new material*
- 20 - *Fig. S2 (old S1): readability improved by changing the LCC colour codes*

(3) SUMMARY OF CHANGES IN RESPONSE TO REVIEW COMMENTS

REFEREE #1

5 MAJOR COMMENTS

1.) constant flux rates: I was extremely surprised when reading the results section to find that temporal variability in flux rates is ignored, instead a constant flux rate is assigned to each of the chosen LCC groups. This constitutes an over-simplification of the tundra ecosystem in the first place, but also limits the presented approach to extremely basic overall findings. Considering that fluxes over a period of 8 weeks from the late growing season of an Arctic ecosystem are used, besides short and mid-term climate variability the fluxes will be influenced by slowly varying conditions such as e.g. thaw depth or soil temperatures. Accordingly, it cannot be assumed that even mean flux levels for moving windows remain constant over such a long period. Even more important in this context, I would strongly assume that the different LCC groups will show a different trend in phenology in this part of the season, i.e. some may be subject to earlier senescence, and also some of them may react more strongly to environmental stress such as water limitation, or first nights with freezing temperatures. This implies that the differences/ratios between flux rates from LCC groups will not be constant over time. So what is the value of providing just a single mean flux rate per LCC group? Would the differences still be significant if short-term temporal variability, and shifts in flux rate ratios, would be taken into account? Regarding the applicability of the results, under the given circumstances the output of the flux decomposition is of no value for any other purpose than investigating a potential sensor location bias (and even here the impact is limited). To reach a broader audience, temporally varying fluxes per biome with functional links to environmental controls would have to be provided. Summarising this item, it is obvious that the chosen approach is based on a strong simplification of the actual flux patterns. This should be discussed in detail in a revised version of the manuscript. This discussion needs to be supplemented by a demonstration how variable measured net flux rates are over time, broken up into the chosen LCC groups. If it cannot be proven that the ratios between flux rates from different groups remain largely constant over time, the approach cannot be applied as is. In general, I strongly urge the authors to consider extending their approach, so temporal variability in flux rates can be considered.

35

Reply: *We extended the discussion of our results substantially, showing that the short-term CH₄ flux variations are mainly generated by footprint variations rather than other environmental controls (Sect. 3.2). To investigate the seasonal trend, we performed a new analysis in which weekly data were used in addition to the full eight-week period. These results were added to the manuscript, including a new figure (Fig. 6) and related discussion (Sect. 3.2). In addition, the correlation of methane fluxes with soil temperature, friction velocity and leaf area index was examined, reported and compared with previous studies in the revised version (Sect. 3.2). We also compared the upscaling results obtained from the weekly data with the original estimate (Sect. 3.4).*

2.) uncertainty estimates: The manuscript misses to even discuss some essential sources of uncertainty that influence the given approach, and those few aspects that are treated (e.g. uncertainties in maps) are only covered qualitatively. Even very easy components, such as e.g. assigning an uncertainty to the input flux rates from the EC system, which is then projected onto the modelled LCC flux rates, is missing. Most importantly, there is no uncertainty estimate for the footprint approach. It is obvious that any source weight function can only be an approximation of the actual field of view of the sensor, as many footprint validation studies have shown in the past. In this study, however, footprint simulations are treated as a given fact. There are uncertainties in all the input parameters used to feed the footprint model, there are uncertainties associated with parameterizations/assumptions inherent to the footprint model, and there are uncertainties related to the methodology (e.g. horizontal homogeneity, stationary flow, and so on). For a modified version of this study, the authors need to provide a convincing concept to constrain the uncertainties in computed source weight functions, and how these influence the results obtained by the flux decomposition approach. In addition, the uncertainty concept should, as mentioned above, also involve the flux data uncertainty, and also the uncertainties inherent to the maps used in this study should be involved, and quantified.

20

Reply: *The error estimation procedure and the reported uncertainty estimates were explained in our original reply (bg-2018-155-AC1). We added related discussion to the revised manuscript as part of a new section dealing with methodological issues (Sect. 3.4). We also added here a paragraph on the uncertainties associated with footprint modelling, citing several validation studies that demonstrate the performance of the model used in our study. Concerning the measurement errors, we added an uncertainty estimate for the mean methane flux (Sects. 2.3.1, 3.3; Fig. 7).*

3.) Validation of flux rates: In Section 3.2, the authors include a good paragraph (p.16 ll.20ff) that supports the negative flux rates found for bare soil. As part of the line of argumentation, chamber measurements from a previous study are cited. I think it's fair to assume that this study did not only measure those 32 data points cited here for bare soil, but also other components within the Tiksi landscape. Why are those not used? Having flux chamber results for the different LCC groups would be the best way to validate that the flux composition actually produced realistic results. Also, the Tiksi flux tower has been running for several years now - why restrict this study to just 8 weeks? Why not use more data, so the database is more representative, and can also resolve temporal variability? Why not split the dataset into training and validation sets, so any finding can actually be evaluated?

40 **Reply:** *The coverage of the flux chamber measurements that are available from Tiksi was explained in our original reply (bg-2018-155-AC1). In the revised version, we include all the chamber data that we consider useful for the present study (Sect. 3.2). These data are now described in Sect. 2.1.2. The study period was*

motivated and the validation procedure explained in our original reply (bg-2018-155-AC1). We revised the Introduction to highlight the scope of the manuscript.

4.) scope of this study: With the limitations of the chosen concept (constant fluxes)
5 as mentioned above, the authors should clearly restrict the scope of the study to an
estimate to constrain sensor location bias. I do not see any other application of their
method besides this (I would be glad to get convinced otherwise, e.g. by a thorough
discussion ..). I do not think they can claim to provide land cover specific CH₄ flux rates,
10 since they present one set of mean flux rates for a single period of time, nothing more.
They also do not interpret EC data, since obviously there's no temporal variability, no
links to environmental controls, no interpretation why certain LCC groups show different
fluxes than others. What is being provided here is an extremely simplified approach to
15 estimate flux rates per LCC group, and check if, given these flux rates, the net fluxes
represent the emissions from a larger area (aka sensor location bias). Since there
is also no discussion which aspects influence the performance of this approach (e.g.
length scale of variability in terrain features, differences in flux rates between LCC
groups, footprint variability, etc), there is no way of telling if this approach could be
applied at other sites as well.

20 **Reply:** *We explained the rationale of the manuscript in the original reply (bg-2018-155-AC1) and clarified it in
the Introduction of the revised manuscript. For the revision, we performed a more detailed analysis of the LCC
group-specific fluxes and investigated their temporal variation and environmental responses (Sect. 3.2). We
added a new section that includes a discussion on the feasibility of the statistical method presented and the
uncertainties involved (Sect. 3.4).*

25 5.) a thorough discussion is simply missing! What is the implication of the findings?
How could the presented approach be used? Where are the weaknesses, which factors
limit the interpretation of the findings?

30 **Reply:** *We added a significant amount of new discussion to the revised version (Sect. 3.2). We also added a new
section that deals with methodological issues, including the applicability and weaknesses of the approach
presented (Sect. 3.4). We reorganized the Conclusions to focus on the key implications of the study.*

GENERAL COMMENTS

35 1.) The introduction is well structured overall, and the 3 different sets of objectives are clearly formulated. The paragraph on methane (starting p.2
l.25) is rather confusing, though, and should be revised.

Reply: *This paragraph was shortened and rephrased.*

2.) Section 2.2 needs a complete overhaul. Many sections, e.g. most parts of 2.2.1, are textbook knowledge, and do not need to be shown in detail herein. Section 2.2.2 is much too detailed for what actually needs to be described. You project a source weight function on gridded maps, and accumulate the weights of individual cells, sorted by categories, nothing more. Overall, this whole section is much too long. I suggest to revise it to the following structure: - 2.2.3 should be moved to the front - 2.2.2 should be shortened, and simplified, coming next - 2.2.1 should be discarded entirely - 2.2.4 should be moved as part of the results section

10

Reply: *In the revised version, Sect. 2.2.1 is removed and a shortened version is included in the Supplement. The rationale of Sect. 2.2.2 was explained in our original reply (bg-2018-155-AC1).*

3.) In Section 2.3, the ordering of the information should be revised. Many pieces of information given in 2.3.2 were needed to interpret the text in 2.3.1, for example

15

Reply: *We made some minor additions to Sect. 2.3.1 to improve the interpretation.*

4.) Results Section 3.1: The first part on general footprint characteristics should be removed (P1, P2). After all, what you basically state here is the obvious fact that footprint areas grow with stable stratification. The authors may move Table 3 to the appendix, and refer to it in the main text in case any reader wants to see the details, but this is clearly not part of the main story. The center part, highlighting the heterogeneity of surface characteristics within the footprint, reads well (P3-P5). The last part (P6+) should be revised - it is informative to describe a sensor location bias using the different surface characteristics, but the current format is confusing, using too many versions of a reference area (also Table 4 should be reduced).

20

25

Reply: *Most of the first part of Sect. 3.1 was removed. Table 3 was moved to the Supplement and briefly cited in the revised Sect. 3.1. In the latter part of this section, the number of different reference areas was reduced and Table 4 was simplified considerably.*

30

4.) p.16 l.10ff: I don't think it makes much sense to compare the Tiksi flux rates against values from other sites without also comparing environmental conditions, and the measurement approaches

35

Reply: *We improved the presentation of this comparison. For the rationale of the comparison, please see our original reply (bg-2018-155-AC1).*

5.) results section 3.3: It is confusing, and actually not understandable, why so many different reference areas have been used to compare the footprint LCC composition to.

40

5 This actually leaves the impression that the authors were searching for a nice configuration that can demonstrate that the EC measurements are actually well representative (e.g. p.17 l.27 ' the sensor location bias could be minimized by reducing the radius to 800– 1000 m'). What is the value in such an exercise? People who are interested in using EC data want to know how well they represent a LARGE area.

Reply: In the revised version, we analyse fewer reference areas (Sect. 3.3, Tables 4 and 6). We also clarified the related presentation (Sects. 3.3, 4). Please see also our original reply (bg-2018-155-AC1).

10

TECHNICAL COMMENTS

p.3 l. 16: I don't see a connection between spatial heterogeneity and the need for long-term measurements . . . ??

15

Reply: This sentence was rephrased.

Section 2.1.1: A bit too brief. Soil types could be mentioned, and it should be mentioned that vegetation is given in a different subsection.

20

Reply: This section was extended, including the suggested material.

Section 2.1.2: The outline of the QC is too short. What exactly was done regarding instationarity, for example? How were unphysical outliers defined? And how were the gaps treated in the end?

25

Reply: This section was revised, including the suggested material.

Section 2.1.3: I suggest moving the definition of PCTs into a table. It should be mentioned that the dominant vegetation, and other characteristics, are described later in 2.1.4

30

Reply: A new table summarizing the LCC properties was included (Table 1). A reference to Sect. 2.1.4 was added to Sect. 2.1.1.

35

p.6 l.16: The authors should decide if they want to use LCC or PCT as a term for this classification. Using both is very confusing!

Reply: The terminology was unified.

40

Fig.4: the lower 3 panels are not necessary , since they show the same patterns as above, only normalized against the black dashed line

Reply: The lower panels were removed, and corresponding right axes were added to the upper figures.

45

REFeree #2

5 The manuscript by Tuovinen et al. aims to use a detailed footprint analysis of a flux tower in Northeast Siberia to identify sensor location bias, while making use of high resolution satellite imagery. I think this study is interesting but, like the other referee, I think this paper could be a lot more effective. I agree with much of what is said in the other review, but I have a few additional comments.

10 First of all: if sensor location bias is your main goal, this can be done a lot easier through an analysis of the land cover classification from the satellite image. The heterogeneity of the landscape is already captured in there, and by taking the average of a hypothetical footprint area at random points within the satellite image, it can be clarified
15 which locations resemble the larger area the most. A rough estimate of the footprint would be required but this would be a lot simpler than the approach in the paper.

Reply: *Please see our original reply (bg-2018-155-AC2).*

20 As for the footprint area itself: the choice of the Korman and Meixner model is curious. There have been many advances in footprint analysis since, see for example Kljun et al (2015) who described a two-dimensional footprint model that already gives the footprint contribution for each part of the footprint. The model is freely available at
25 <http://footprint.kljun.net> for Matlab, R and python.

Reply: *We added discussion on the uncertainties related to footprint modelling, citing relevant validation studies. Please see also our original reply (bg-2018-155-AC2).*

30 If the authors had used this model, they could have simplified a large part of the methods, which would really help with the readability of the paper. At present, the long list of equations makes it hard to follow what the direction of the paper is, especially since many of them are not referred to later on. Like the author referee said, we don't need textbook knowledge. Sections 2.1 and 2.2 should be drastically shortened to only those equations directly relevant to the paper.

35 **Reply:** *We removed Sect. 2.2.1 and added a shortened version to the Supplement. Please see also the original replies (bg-2018-155-AC1, bg-2018-155-AC2).*

40 Also, I don't understand why there are not more flux chamber measurements in the area, but only from bare soil. The spatial heterogeneity of methane fluxes can be much better identified from direct measurements rather than the inverse method presented here.

Reply: *The coverage of the flux chamber measurements that are available from Tiksi was explained in our original reply (bg-2018-155-AC2). In the revised version, we include all the chamber data that we consider useful for the present study (Sect. 3.2). These data are now described in Sect. 2.1.2.*

- 5 Please, when reporting EC methane flux measurements, use nmol/m²/s rather than micrograms.

Reply: *Please see our original reply (bg-2018-155-AC2).*

- 10 Finally, the authors should put their research in a better context compared to existing literature. The discussion is very limited, and previous studies that have had detailed footprint analyses or emphasized the spatial variation of methane fluxes are either ignored or referenced too briefly. See for example Matthes et al (2014) and Maruschak et al (2016) for two prime examples, but also the paper by Parmentier et al. (2011) which
15 you do cite but without mentioning that it also dealt with methane flux heterogeneity. There are many more, and this needs to be recognized.

Reply: *We enhanced the discussion of our results in Sect. 3.2 considerably and added a new section (Sect. 3.4). The literature considered in the manuscript was extended significantly, including the references suggested here;*

- 20 *especially the paper by Parmentier et al. (2011) is discussed in the revised version.*

Other comments:

- Page 2, line 27: it would make more sense to mention only natural emissions, since
25 this paper focuses on that. This number of 560 Tg/yr is anthropogenic plus natural.

Reply: *The proportion of natural emissions was added to this sentence.*

- Page 3, line 13-15: this has been known for decades, and should not be presented as
30 something new. See for example Christensen, 1993; Torn and Chapin, 1993; Whiting and Chanton, 1992.

Reply: *This sentence was removed for clarity.*

- 35 Page 5, line 27-28: a table with vegetation descriptions for each class would be helpful.

Reply: *Such a table was added (Table 1).*

- Page 6, line 9: have you considered NDWI as another wetness index?

40

Reply: *Please see our original reply (bg-2018-155-AC2).*

Page 10, line 23: is this normalization necessary? This paragraph seems like a com-

plex way of simply saying that you have some unknown data in your average. In any case, at 1.4 km from the tower the effect would be negligible.

Reply: *Please see our original reply (bg-2018-155-AC2).*

5
Page 12, line 23: which Eriophorum species? Not all of them are high emitters of methane, like Eriophorum vaginatum.

Reply: *'e.g., E. vaginatum' was added to the text.*

10
Page 15, line 6-7: "the areal coverage of the LCC within the study area"? what do you mean? The LCC map?

Reply: *This was corrected to 'LCCs'.*

15
Page 17, line 27: this feels like cheating. The tower is not representative for the larger region, so you reduce the region. Please don't.

Reply: *We rephrased these sentences to clarify our presentation.*

20
Page 18, line 2: there's no doubt that lakes are a significant source of methane in the Arctic. Please rewrite this sentence to remove the suggestion that it may not be (e.g. 'Nevertheless, Arctic lakes and ponds emit significant amounts of CH₄ in general).

25
Reply: *We corrected this sentence by removing 'may'.*

Page 31, figure 1. Please don't use a continuous color map for land cover. Use discrete colors.

30
Reply: *We changed the colour codes in Fig. 1a (and a corresponding LCC map in Fig. S2) to improve the readability.*

35
(4) MARKED-UP MANUSCRIPT

Interpreting eddy covariance data from heterogeneous Siberian tundra: land cover-specific methane fluxes and spatial representativeness

5 Juha-Pekka Tuovinen¹, Mika Aurela¹, Juha Hatakka¹, Aleksi Räsänen^{2,3}, Tarmo Virtanen², Juha Mikola⁴, Viktor Ivakhov⁵, Vladimir Kondratyev⁶, Tuomas Laurila¹

¹Finnish Meteorological Institute, Climate System Research, P.O. Box 503, FI-00101 Helsinki, Finland

²Ecosystems and Environment Research Programme, Faculty of Biological and Environmental Sciences and Helsinki Institute of Sustainability Science (HELSUS), P.O. Box 65, FI-00014 University of Helsinki, Finland

³Department of Geography, Norwegian University of Science and Technology, NO-7491 Trondheim, Norway

10 ⁴Ecosystems and Environment Research Programme, Faculty of Biological and Environmental Sciences, University of Helsinki, Niemenkatu 73, FI-15140 Lahti, Finland

⁵Voieikov Main Geophysical Observatory, St Petersburg, Russia

⁶Yakutian Service for Hydrometeorology and Environmental Monitoring, Tiksi, Russia

Correspondence to: Juha-Pekka Tuovinen (juha-pekka.tuovinen@fmi.fi)

15 **Abstract.** The non-uniform spatial integration, ~~an~~ inherent ~~feature of~~ the eddy covariance (EC) method, ~~creates~~ ~~provides~~ ~~an~~ ~~additional~~ challenge for ~~flux~~ data interpretation ~~when fluxes are measured~~ in a heterogeneous environment, ~~as~~ ~~where~~ the contribution of different ~~land coversurface~~ types varies with flow conditions, potentially resulting in ~~a~~ ~~biased~~ ~~estimates~~ ~~in~~ ~~comparison~~ ~~to~~ ~~the~~ ~~as~~ ~~compared~~ ~~to~~ ~~the~~ ~~true~~ areally averaged fluxes and ~~land coversurface~~ attributes. We modelled flux footprints and characterized the spatial scale of our EC measurements at Tiksi, a tundra site in northern Siberia, ~~including a~~ ~~comparison~~ ~~of~~ ~~different~~ ~~source~~ ~~area~~ ~~definitions~~. We used leaf area index (LAI) and land cover class (LCC) data, derived from very high spatial resolution satellite imagery and field surveys, and quantified the sensor location bias. We found that methane (CH₄) fluxes varied strongly with wind direction (~~from~~ -0.09 to 0.59 μg CH₄ m⁻² s⁻¹ on average) ~~during summer 2014~~, reflecting the distribution of different LCCs. ~~Other environmental factors had only a minor effect on short-term flux variations but influenced the seasonal trend~~. Using footprint weights of grouped LCCs as explanatory variables for the measured CH₄ flux, we ~~then~~ developed a multiple regression model to estimate LCC ~~group~~-specific fluxes. This model showed that wet fen and graminoid tundra patches in locations with ~~a~~ ~~high~~ topography-~~enhanced~~ ~~based~~ wetness-~~index~~ acted as strong-~~CH₄~~ sources (1.0-0.95 μg CH₄ m⁻² s⁻¹ ~~during the peak emission period~~), while mineral soils were significant sinks (-0.13 μg CH₄ m⁻² s⁻¹). ~~Finally,~~ ~~to~~ assess the representativeness of ~~CH₄ flux~~ measurements, we upscaled the LCC ~~group~~-specific fluxes to different spatial scales. ~~This assessment showed that,~~ ~~d~~Despite the ~~landscapesurface~~ heterogeneity and rather poor representativeness of EC data with respect to the areally averaged LAI and coverage of some LCCs, the mean ~~CH₄ flux measured during summer 2014~~ was close to the ~~CH₄~~ ~~corresponding~~ balance upscaled to an area of 6.3 km², with a location bias of 14 %. We recommend that EC site descriptions in a heterogeneous environment should be complemented with footprint-weighted high-resolution data on vegetation and other ~~relevant~~ site characteristics.

20

25

30

1 Introduction

Biosphere–atmosphere exchange of greenhouse gases (GHGs) is commonly measured using the micrometeorological eddy covariance (EC) method (Aubinet et al., 2012). This tower-based, non-intrusive technique provides spatially integrated flux data at the ecosystem scale with a typical integration domain of a few hectares. This is in stark contrast to flux chamber measurements that can be focused on homogeneous small-scale ($< 1 \text{ m}^2$) patches of an ecosystem or on individual plant communities (Livingston and Hutchinson, 1995; Virkkala et al., 2017). The spatial aggregation inherent in the EC data is a strong asset if one’s objective is to study functioning or GHG exchange of an extensive, relatively homogeneous ecosystem. Heterogeneous landscapes consisting of a mosaic of differing vegetation and land cover patches, however, may entail issues on the interpretation of the spatial representativeness of measurements. This stems from the fact that the EC integration process equals to non-uniform weighting of the upwind surface elements that influence the measured flux, thus potentially resulting in an unequal and temporally varying contribution from different land surface cover types (Schmid, 2002). Especially isolated zones of high source/sink density may bias the estimated average flux of the area surrounding the EC tower. The spatial distribution of relative weights, a function that Leclerc and Thurtell (1990) coined “footprint”, depends on the measurement height and strongly on wind direction. As the flux footprint is also affected by other properties of the atmospheric flow, e.g., hydrostatic stability, directional averaging does not guarantee an unbiased flux estimate either.

Arctic tundra serves as a prime example of a surface that is heterogeneous with respect to biogeochemical processes. The vegetation, soil and land cover structure of tundra areas are fragmented, the landscape typically comprising patches of different plant communities, water bodies and other land cover types (Stow et al., 2004; Virtanen and Ek, 2014; Mikola et al., 2018). Such heterogeneity concerns both the composition and configuration of land cover surface properties. This is clearly manifested by the leaf area index (LAI), which shows a higher relative variation among sites in tundra than in any other biome (Asner et al., 2003), and there are ~~also~~ pronounced spatial and temporal LAI patterns at the landscape scale (Marushchak et al., 2013; Juutinen et al., 2017).

Surface heterogeneity ~~can also~~ generates high variability in the ecosystem–atmosphere fluxes of GHGs, including methane (CH_4) ~~fluxes~~ (Olefeldt et al., 2013). ~~Methane is a potent GHG that is accumulating in the atmosphere, and t~~ Tundra biomes are responsible for ~~ca. about~~ 3 % of the total CH_4 emissions estimated at 560 Tg yr^{-1} , 40 % of which is biogenic (McGuire et al., 2012; Saunois et al., 2016). The emissions from tundra are predicted to increase substantially, as a fraction of the permafrost soils contain vast reservoir amounts of organic carbon in permafrost soils (approximately 1000 Pg in $0\text{--}3 \text{ m}$ depth; ~~Hugelius et al., 2014~~) and a fraction of this may be released into the atmosphere as a result of warming-induced thawing ~~of these soils~~ (Schuur et al., 2015). ~~While the processes involved are incompletely understood, with large uncertainties in the estimated increase in CH_4 production (Cooper et al., 2017; Mård et al., 2017), these emissions potentially enhance surface warming, thus~~ creating a positive feedback to climate change (Schuur et al., 2015; ~~Nzotungieimpaye and Zickfeld, 2017~~).

The heterogeneity in the ~~land-surface ecosystem~~–atmosphere CH₄ flux originates from the multitude of biochemical and physical controls of the anaerobic CH₄ production and bacterial CH₄ oxidation (Whalen and Reeburgh, 1990; Lai, 2009; Bridgman et al., 2013). Methane can be released into the atmosphere through gradual diffusion in soil and water, in ebullition (bubbling) events and via plant-mediated advective transport. These processes involve different residence times and thus expose the produced CH₄ to different degree of oxidation. As a result of this complexity, field studies have identified a wide range of factors that are associated with the levels and variations of observed fluxes. Of these, soil temperature and moisture (or water table level) typically constitute the key environmental controls (Olefeldt et al., 2013). As a general rule, wet carbon-rich soils emit substantial amounts of CH₄, while dry tundra soils act as small net sinks (Lau et al., 2015). ~~Even if lesser in magnitude, the uptake flux in dry areas may dominate the regional CH₄ balance (Jørgensen et al., 2015; D’Imperio et al., 2017). Methane flux strongly depends on vegetation and soil characteristics, such as the abundance of vascular plants with aerenchyma tissue facilitating gas transport; other important variables include substrate availability, and soil acidity and redox potential (Lai, 2009; Bridgman et al., 2013; Olefeldt et al., 2013). The key role of vegetation type was convincingly demonstrated by Davidson et al. (2016), whose simple vegetation classification could explain CH₄ emissions from Arctic tundra as accurately as the key environmental drivers.~~

Landscape heterogeneity not only calls for further ~~long-term~~ measurements of fluxes and their controls on multiple spatial scales, preferably including multiple EC towers for spatial replication (Hill et al., 2017), but also necessitates development of techniques for data interpretation, including down- and upscaling methods ~~required~~ for generalization of observations. Micrometeorological models are available for estimating the flux footprint (Leclerc and Foken, 2014), and ~~these models~~ have been utilized in various ways when dealing with the representativeness of flux measurements, based on either chambers or EC, or a combination of the two. In its simplest form, such an analysis involves determination of footprint dimensions for typical flow conditions, to ensure that the expected “field of view” of EC measurements is sufficiently confined to the area of interest (e.g., Aurela et al., 2009), or to roughly evaluate the appropriate upscaling area of chamber measurements that are compared with concurrent EC data (e.g., Riutta et al., 2007).

Averaged footprints, or footprint “climatologies”, can be calculated from time series of actual short-term (typically 30 min) meteorological data, thus providing a fuller view of the spatial extent of EC aggregation (e.g., Amiro, 1998). A flux-weighted footprint climatology has been suggested for further illustration, hinging on the assumption that the surface flux is spatially uniform within each short-term footprint (Chen et al., 2009). When combined with a land cover map, footprint time series can be used for data quality control by quantifying the contribution of different land cover types or, specifically, that of a certain ecosystem intended to be observed (Tuovinen et al., 1998; Rebmann et al., 2005; Göckede et al., 2008). The footprint function can also be used for a formal expression of the spatial, or more precisely the point-to-area (Nappo et al., 1982), representativeness of the EC measurements performed at a certain location. A suitable metric for this, termed the

“sensor location bias” by Schmid and Lloyd (1999), can be defined by comparing the footprint-weighted average of a surface-related quantity, mapped across the study area, to the corresponding arithmetic average.

5 While EC data from a heterogeneous environment are still commonly compared with plot-scale data without considering the differential weighting of the plots in the EC signal (e.g., Heikkinen et al., 2002; Sachs et al., 2010; Yu et al., 2013), footprint modelling has been successfully combined with land cover information in various studies for a representative upscaling of chamber-based fluxes (e.g., Marushchak et al., 2016), plot-scale model results (e.g., Budishchev et al., 2014), remotely sensed fluxes (e.g., Chen et al., 2009) and vegetation data for model input (e.g., Stoy et al., 2013). The temporally varying footprint weights of different land cover types can also be taken as a basis for constructing statistical models ~~that~~ unravel
10 land cover-specific fluxes ~~estimates~~ from the spatially aggregated EC data, but this depends on the quality of land cover data (Fan et al., 1992; Forbrich et al., 2011). The very high spatial resolution (VHSR) satellite imagery makes it possible to derive reliable land cover maps with as high as a ~1 m resolution. By utilizing such a detailed vegetation map, Budishchev et al. (2014) showed that footprint-weighting of modelled plot-scale CH₄ emissions from permafrost tundra resulted in a good agreement with EC measurements, while areally averaged fluxes failed to reproduce the heterogeneity-induced temporal
15 variability. A similar conclusion was reached by Davidson et al. (2017), who upscaled chamber-based CH₄ fluxes for four sites in Alaska by means of VHSR vegetation maps.

The aims of the present study are threefold. First, we characterize the dimensions of the field of view and the point-to-area representativeness of the EC measurements carried out at a micrometeorological measurement station, located on permafrost
20 tundra at Tiksi in northern Siberia, during summer 2014. We demonstrate and quantify the heterogeneity of this site, producing information that is essential for any further study exploiting these flux data. For this we employ a micrometeorological footprint model and detailed maps of ecosystem surface characteristics, including land cover classes (LCCs), ~~and~~ LAI and topographic wetness index (TWI). These are based on VHSR satellite imagery and extensive field surveys, which still are scant for Siberian tundra; ~~in addition, we utilize the topographic wetness index (TWI) derived from a~~
25 VHSR digital elevation model. Second, we hypothesize that distinguishable mean fluxes can be determined for LCC groups that represent different CH₄ source/sink capacities; this can be accomplished by developing a multiple regression model that links these fluxes to the EC measurements via footprint weighting. This approach was motivated by the findings of Davidson et al. (2016), who demonstrated that a simple vegetation classification could explain the variation in CH₄ emissions from
30 Arctic tundra as accurately as a set of key environmental drivers. Furthermore, the flux and the chamber measurements made at Tiksi our site that showed that the effect of surface type-LCC was much larger than that of environmental controls (Vähä, 2016). Because of this objective, we limit our data to the growing season. Finally, the LCC group-specific fluxes obtained in this way offer us an opportunity to upscale the CH₄ balance to the landscape scale and thus to evaluate the representativeness of EC measurements also with respect to CH₄ exchange. We emphasize that the scope of this study is focused on the

ramifications of the unavoidable non-uniform spatial sampling involved in EC measurements rather than on ecosystem processes.

2 Material and methods

2.1 Site and data

5 2.1.1 Site description and meteorological conditions

The study area covers the surroundings of the micrometeorological GHG flux measurement station at Tiksi in northeastern Russia, near the Tiksi Observatory operated by Yakutian Service for Hydrometeorology and Environmental Monitoring. The EC tower of the station is located at 71.5943°N, 128.8878°E, 7 m above sea level, ca. about 500 m from the shoreline of the Laptev Sea, and ca. 50 km from~~close to~~ the Lena River delta. The site-flux measurements are~~is~~ run by the Finnish Meteorological Institute and constitute~~is~~ part of the International Arctic Systems for Observing the Atmosphere (IASOA) activities (Uttal et al., 2016).

Tiksi is located within the continuous permafrost zone, and the climate is arctic: the winters are long and cold, while the summers are cool. The mean annual temperature and precipitation at Tiksi in 1981–2010 were -12.7 °C and 323 mm, respectively; the year 2014 was somewhat warmer (-10.9 °C) and drier (249 mm) (AARI, 2018). Air temperature typically falls below 0 °C in the end of September, and the soil temperatures reach the freezing point at approximately the same time. During the winter, air temperatures are typically below -20 °C, and the soil temperatures are reduced to levels below -10 °C. Snow appears typically in October and melts in early June. After the snowmelt, the top (a few cm) layer of soil warms quickly, but the thawing rate of deeper layers varies depending on the soil type and vegetation (Mikola et al., 2018). ~~The study area is within the continuous permafrost zone; the depth of the active soil layer typically varied within 0.2–0.4 m in early July—mid August 2014 (Mikola et al., 2018).~~

The soil type ranges from mineral soil to peatlands with a high organic content (>60 % of dry soil mass) (Mikola et al., 2018). The landscape around the EC tower represents the coastal tundra zone of eastern Siberia with a high diversity of plant species and community typesies, including fens, bogs, tundra heaths and meadows, but there are also areas of bare ground (Nyman, 2015; Juutinen et al., 2017; Mikola et al., 2018). The terrain is relatively flat, sloping gently (2 – 3 °) towards the south. This generates a hydrological gradient, and ~~there is~~ a small brook runing through the ~~study area site~~; there are also ponds and small lakes within the study area. Further details of vegetation and soil characteristics are presented in Sects. 2.1.3 and 2.1.4.

The data analysed in this study cover the period of 5 July to 29 August 2014, which represents the thermal growing season of that year, using the daily mean air temperature of 5 °C as the threshold (Fig. S1 in the Supplement). During this period, the mean air temperature was higher (10.2 °C) than the corresponding 1981–2010 mean (7.8 °C), which was also the case for the precipitation sum (116 mm vs. the long-term mean 86 mm). In 2014, the soil temperature at 10 cm depth varied within the typical summertime range of 5 ± 2 °C from early July to the end of August. The depth of the active soil layer mostly varied within 0.2–0.4 m in early July – mid-August 2014 (Mikola et al., 2018).

2.1.2 Eddy covariance data Flux measurements

The CH₄ and energy fluxes used in the present study were measured continuously with the micrometeorological eddy covariance method (Aubinet et al., 2012). The EC instrumentation consisted of a USA-1 (METEK GmbH, Elmshorn, Germany) sonic anemometer/thermometer, an LI-7000 (LI-COR, Inc., Lincoln, NE, USA) CO₂/H₂O analyser and an RMT-200 (Los Gatos Research, Inc., San Jose, CA, USA) CH₄ analyser. The measurement height was 3 m. The sampling frequency was 10 Hz, and the turbulent fluxes were calculated with the in-house PyBARFluxCalc program with 30 min block averaging according to standard procedures, including double coordinate rotation, lag determination, and wet-to-dry mole fraction conversion ~~and high frequency flux loss correction~~ where necessary (Aubinet et al., 2012). The high-frequency CH₄ flux loss was corrected for using an empirical approach described by Laurila et al. (2005); for this a half-power frequency of 1.1 Hz was estimated from the data. The CH₄ flux data were screened for instationarity by removing cases in which the relative non-stationarity of either momentum or CH₄ flux exceeded 30 % (Foken and Wichura, 1996). In addition, periods of weak turbulence (friction velocity < 0.12 m s⁻¹) were discarded and unphysical outliers. No gap-filling of the time series was necessary for the purposes of the present study. ~~The CH₄ flux data analysed in the present study cover the period of 5 July to 29 August 2014, which represents the thermal growing season of that year, using the daily mean air temperature of 5 °C as the threshold.~~

In addition to the EC technique, CH₄ exchange was measured with a static flux chamber (Vähä, 2016). The surface area of this chamber was 0.25 m² and its height 0.3 m. The sample air from the chamber was directed to a DLT-100 (Los Gatos Research, Inc., San Jose, CA, USA) CH₄ analyser. The chamber closure time was either 4 or 10 min, depending on the LCC and the expected magnitude of CH₄ flux. The measurements were carried out between 15 July and 16 August 2014. However, the number of chamber plots was modest and the reach of these measurements from the EC mast was limited due to the use of an online gas analyser; moreover, the measurement plots do not fully correspond to the land cover classification that was developed subsequently (Mikola et al., 2018) and used in the present study. Therefore, instead of aiming at a full analysis of the chamber data, we utilized them for a partial validation of the estimated LCC-specific fluxes, using four plots on dry fen, two plots on wet fen and one plot on bare soil, with 31 or 32 measurements taken on each plot.

2.1.3 ~~Surface Mapping of landscape characteristics~~ mapping

The land cover classification ~~consists of was based on seven~~ nine classes visually distinguished according to their key characteristics (Table 1) ~~judged plant community types (PCTs) augmented by two non-vegetated surfaces: (1) wet fen, (2) dry fen, (3) bog, (4) graminoid tundra, (5) flood meadow, (6) shrub tundra, (7) lichen tundra, (8) bare ground and (9) water~~ (Mikola et al., 2018). The ~~PCTs-LCCs~~ were identified within an area of 1 km² around the EC tower on the basis of ~~an~~ extensive a vegetation and soil survey. ~~They were and~~ verified using statistical ordination of the 92 established study plots according to plant species composition and functional plant and soil attributes (Mikola et al., 2018). To extrapolate the LCCs to the landscape scale (Fig. 1a, Fig. S24 in the Supplement), a supervised object-based ~~random forest~~ classification with the random forest method was carried out using two VHSR multispectral satellite images (12 August 2012 and 11 July 2015; WorldView-2, DigitalGlobe, Inc., Westminster, CO, USA) and a digital elevation model (DEM) constructed from the 2015 WorldView-2 stereo pair (Fig. 1b). The internal (cross-validation of training data) and external (validation data) classification accuracy of the land cover classification were 80 and 49 %, respectively. For details, see Mikola et al. (2018).

Using non-linear regression, the LAI of vascular plants was estimated from the normalized difference vegetation index (NDVI) calculated from the reflectance data of the 2012 WorldView-2 image (Fig. 1c). This map, which represents the period of maximum LAI in 2012; for the estimated development of the LAI of different LCCs in 2014, see (Juutinen et al., 2017; ~~Fig. 4e~~) and Fig. S1 (in the Supplement). The topographic wetness index (TWI) was calculated from the DEM using the method of Böhner and Selige (2006) (Fig. 1d). TWI is defined as a function of the upslope contributing area and the local terrain slope, and thus ~~it~~ serves as a proxy for potential soil moisture. For details of the DEM and TWI data, see Mikola et al. (2018). All maps have a 2 m pixel size, and in this study they were limited to a circle with a radius of 1.4 km from the EC tower, which defines the domain of the present study. For upscaling to a regional scale, we also considered ed the LCCs determined within a larger area of 35.8 km² (Fig. S24 in the Supplement).

2.1.4 Main features of the land cover classes

The LCCs employed in the present study are described by Juutinen et al. (2017) and in greater detail by Mikola et al. (2018); a summary of observed vegetation characteristics is provided in Table 1. Briefly, the dry fen, wet fen and bog classes represent peat-forming environments, while the other LCCs refer to surfaces that have environments with no discernible peat layer. The vascular plant vegetation of fens, i.e. the wetter peatlands, is characterized by sedges (*Carex* spp.). In 2014, the LAI of this vegetation reached its maximum in early August, estimated at 1.1 and 0.5 for wet and dry fens, respectively (Fig. S1 in the Supplement; Juutinen et al., 2017). ~~Sphagnum and feather~~ mosses are abundant in the dry fens, while in the wet fens the moss cover ~~of wet fens~~ is sparse and water pools are common. The bogs are drier and show microtopographic variation; ~~and~~ their vegetation ~~is dominated by~~ consists mainly of dwarf shrubs, dwarf birch (*Betula nana*), and *Sphagnum* and ~~other feather~~ mosses. The vegetation of flood meadows and graminoid tundra is dominated by graminoids (sedges and

grasses) and willows (*Salix* spp.), which yield a relatively high maximum vascular-plant LAI of 0.9 and 0.7, respectively, for these LCCs during the study period (Juutinen et al., 2017). The areas defined as shrub tundra have an abundant coverage of feather mosses and dwarf shrubs. In addition, lichen tundra patches with lesser biomass alternate with stony bare-ground areassurfaces.

In terms of soil properties of the vegetated areassurfaces, the dry fen, wet fen, bog and graminoid tundra LCCs stand out with their high organic matter (on average 38 % of soil dry mass) and water concentration (on average 73 % of fresh mass) in the top 10 cm soil layer, while the lowest concentrations (4 and 22 %, respectively) were found in the soils of the lichen tundra LCC, as measured on 9–14 August 2014 (Mikola et al., 2018). The soil temperature at a depth of 15 cm was clearly highest in the lichen tundra sampling plots, and flood meadow and wet fen soils mostly had a higher temperature than those of the other remaining LCCsecommunity types. The depth of the biologically active soil layer approximately doubled from early July to mid-August 2014 (the period when weekly measurements were taken). In mid-August, the active layer depth was highest, aboutca. 40 cm, at the wet fen and flood meadow plots and lowest, aboutca. 25 cm, at the shrub tundra and lichen tundra plots (Mikola et al., 2018).

2.2 Application of footprints

2.2.1 Footprint function

The footprint function, φ , defines the relationship between the source distribution of a quantity, $Q_{\vec{y}}$, and the value of this quantity, η , at a certain location, \vec{x} . It is defined by the general integral equation (Pasquill and Smith, 1983; Schmid, 2002)

$$\eta(\vec{x}) = \int_{\Omega} \varphi(\vec{x}, \vec{x}') Q_{\vec{y}}(\vec{x}') d\vec{x}', \quad (1)$$

where Ω denotes the integration domain and sinks are understood as negative sources. We assume that φ only depends on the displacement of a source from the reference location, $\vec{x} - \vec{x}'$, and not on this location itself, implying that φ is independent of $Q_{\vec{y}}$; that is, the variable surface forcing is associated with inhomogeneities in a source strength of a passive scalar that do not affect the turbulence field. This is the so-called inverted plume assumption whose validity is a key prerequisite for the applicability of Eq. (1) (Schmid, 2002), which can be interpreted as a superposition of individual solutions for unit point sources, if the equations governing η are linear (Horst and Weil, 1994).

By specifying that the source term represents the horizontal distribution of a scalar flux density (hereafter referred to as “flux”) at the ground surface and by defining the reference location \vec{x} as the point at which the atmospheric vertical flux of this constituent is known, we can define the footprint function specific to this configuration, f , here expressed in polar coordinates, with

$$\langle F \rangle = \int_0^\infty \int_0^{2\pi} f(\theta, r) F(\theta, r) d\theta dr; \quad (2)$$

where F is the surface flux distribution, $\langle F \rangle$ is the vertical flux at a reference location above the surface, and θ and r are the horizontal direction and distance with respect to this location. We assume that f represents a normalized distribution; i.e., $f \in [0,1], \forall \theta, r$, and $\int_0^\infty \int_0^{2\pi} f(\theta, r) d\theta dr = 1$.

5 The flux footprint defined by Eq. (2) provides a means to identify and depict the influence of a two-dimensional surface on a point measurement. However, there are alternative ways of doing this, some of which are formalized here for clarity. Following Schmid (1994), we first define the cumulative footprint, or the source area, Π , in such a way that it corresponds to the smallest bounded region containing the surface elements that contribute to the measurement signal by a specified fraction $P \in (0,1)$. The source area defined in this way is bounded by a footprint isopleth, $f = f_P$, within which the integral of f
10 equals P ;

$$\Pi(f_P) = \int_0^{2\pi} \left(\int_{r_{P,\perp}(\theta)}^{r_{P,z}(\theta)} f(\theta, r) dr \right) d\theta = P, \quad (3)$$

where the direction dependent distances $r_{P,\perp}(\theta)$ and $r_{P,z}(\theta) > r_{P,\perp}(\theta)$ are defined by the condition $f > f_P$, if $r_{P,\perp} < r < r_{P,z}$. This formulation defines an arbitrary area, but it is also possible to derive averaged dimensions in terms of a direction-independent range $r_{P,\perp} - r_{P,z}$, i.e., an annulus, corresponding to a given P , if we first integrate along the angular coordinate,

$$\Pi^*(r_{P,\perp}, r_{P,z}) = \int_{r_{P,\perp}}^{r_{P,z}} \left(\int_0^{2\pi} f(\theta, r) d\theta \right) dr = P, \quad (4)$$

where the distances $r_{P,\perp}$ and $r_{P,z}$ minimize the annular area. (It is assumed here that the footprint distribution makes it
15 possible to define unique $r_{P,\perp}$ and $r_{P,z}$, which is not true for an arbitrary f). Both Eqs. (3) and (4) mean that also the closest edge of the source area, i.e., $r_{P,\perp}$, is located at a distance upwind from the measurement point. While Eq. (3) answers the question “What is the area that contributes most to the measured flux?”, Eq. (4) corresponds to “From which range does the flux originate, on average?”

20 Alternatively, we can set $r_{P,\perp} = 0$ and define the cumulative footprint corresponding to Eqs. (3) and (4) as

$$\Pi_0(f_P) = \int_0^{2\pi} \left(\int_0^{r_P(\theta)} f(\theta, r) dr \right) d\theta = P \quad (5)$$

and

$$\Pi_0^*(r_P) = \int_0^{r_P} \left(\int_0^{2\pi} f(\theta, r) d\theta \right) dr = P, \quad (6)$$

respectively. In Eq. (5), the distance $r_p(\theta)$ coincides with a footprint isopleth. These definitions make it possible to characterize the measurement with a distance that is related to the traditional fetch concept (Dyer, 1963).

The area of influence is also commonly depicted on the basis of the cross-wind integrated footprint, where the integration is performed in Cartesian coordinates simply as

$$\Pi_C(f_P) = \int_0^{x_P} \left(\int_{-\infty}^{\infty} f(x, y) dy \right) dx = P, \quad (7)$$

where x_P is the distance from the mast within which the proportion P of the measured flux originates from, termed the “effective fetch” by Gash (1986). This is a useful definition if f represents stationary conditions, i.e., a single short term period, while Π , Π^* , Π_g and Π_g^* can be meaningfully determined also for the footprint averaged over multiple flow conditions, i.e., for the time averaged f representing a footprint climatology.

2.2.12 Footprint-weighted averaging and sensor location bias

The footprint function (Horst and Weil, 1992) specific to a certain measurement configuration (f) can be expressed in polar coordinates as

$$\langle F \rangle = \int_0^{\infty} \int_0^{2\pi} f(\theta, r) F(\theta, r) d\theta dr, \quad (1)$$

where F is the surface flux density distribution, $\langle F \rangle$ is the vertical flux density at the measurement point above the surface, and θ and r are the horizontal direction and distance with respect to this location. The footprint equation (Eq. 2) Equation (1)

postulates that the flux at a certain location above the ground-surface represents a spatial weighting of the surface flux distribution, where the weighting is defined by the footprint function $f \in [0,1], \forall \theta, r$ & $\int_0^{\infty} \int_0^{2\pi} f(\theta, r) d\theta dr = 1$, that describes the turbulent transport between each surface element and the reference point. In the context of EC measurements, the location of the EC tower defines the origin of the coordinate system (θ, r) , and f is specific to the sensor height and f can be estimated by micrometeorological modelling (Leclerc and Foken, 2014); and $\langle F \rangle$ denotes the measured flux, while typically $F(\theta, r)$ is unknown.

Based on $f(\theta, r)$, we can, analogously to Eq. (12), define footprint-weighted averages of other quantities. For a continuous variable X , such as LAI and terrain elevation, we write this average, or the “effective” value of X related to a certain footprint f , as

$$\langle X \rangle = \int_0^{\infty} \int_0^{2\pi} f(\theta, r) X(\theta, r) d\theta dr. \quad (28)$$

We can ~~also~~ apply a similar averaging operation to an LCC map, in which each location (in practice, a pixel) is allocated to a single LCC. If we denote the LCC map by $\Lambda(\theta, r) = j$, where the integer $j = 1 \dots N$ specifies the LCC at (θ, r) , the weighted LCC corresponding to f is defined as

$$\langle \Lambda \rangle_j = \int_0^\infty \int_0^{2\pi} f(\theta, r) \delta(\Lambda, j) d\theta dr, \quad (39a)$$

where

$$\delta(\Lambda, j) = \begin{cases} 0, & \Lambda(\theta, r) \neq j \\ 1, & \Lambda(\theta, r) = j \end{cases} \quad (39b)$$

5 This provides the proportion of each LCC within the footprint, which can be calculated for a footprint climatology as well as a single footprint distribution. If the variable X in Eq. (28) is LCC-specific but otherwise does not depend on location, i.e., we can specify constants X_j , $j = 1 \dots N$, then we can combine Eqs. (28) and (93) to obtain the footprint-weighted X as

$$\langle X \rangle = \sum_{j=1}^N \int_0^\infty \int_0^{2\pi} f(\theta, r) \delta(\Lambda, j) X_j d\theta dr. \quad (44)$$

To describe the point-to-area representativeness of the flux measurements with respect to a variable related to a surface property or exchange, we follow Schmid and Lloyd (1999) and define a metric that quantifies how well the measurement at a
 10 certain location reflects the actual conditions averaged over the area of interest. The sensor location bias for X is calculated here as

$$\Delta_x = \frac{\langle X \rangle - \bar{X}}{\bar{X}}, \quad (54)$$

where \bar{X} denotes the mean X within the study area. This definition differs from the one introduced by Schmid and Lloyd (1999), who expressed the sensor location bias as Δ_x^2 . As $\langle X \rangle$ depends on the footprint and thus varies with time, Δ_x is not temporally invariant either.

15

We calculated the sensor location bias for terrain elevation, the maximum LAI and TWI that were mapped across the study area (Fig. 1). In addition, to investigate the effect of landscape heterogeneity, this bias was calculated for the mean CH_4 flux, for which the areal reference was obtained from the LCC group-specific fluxes estimated with a multiple regression model (to be described in Sect. 2.3).

20 **2.2.32 Footprint modelling**

We calculated the flux footprints f for each 30 min flux averaging period in a horizontal $2 \text{ m} \times 2 \text{ m}$ grid by using the analytical footprint model developed by Kormann and Meixner (2001) (here “KM model”). The KM model is based on a stationary gradient diffusion formulation, building on the classical solution of the two-dimensional advection–diffusion equation with vertical power law profiles assumed for the mean wind speed and eddy diffusivity (Pasquill and Smith, 1983).

As a novel feature, these profiles are related to the corresponding Monin–Obukhov similarity (MOS) profiles. The crosswind diffusion is assumed to be Gaussian and height-independent.

5 Our EC measurements provide the necessary input data for the KM model, including mean wind direction θ , mean horizontal wind speed (at anemometer height), U , friction velocity u_* , hydrostatic stability $(L^{-1})L^{-1}$, and the standard deviation of lateral wind velocity $(\sigma_v)\sigma_v$. When matching the wind and diffusivity power laws to the MOS profiles at the measurement height, the KM model does not require an explicit definition of roughness length $(z_0)z_0$, since the input data (i.e., U , u_* , L^{-1}) implicitly specify z_0 according to the MOS profile of the horizontal wind speed. In the case of a heterogeneous surface, this simplifies the computations significantly as compared to models that require additional flux aggregation procedures for estimating the effective z_0 (Göckede et al., 2006).

Independent of the flow conditions, a part of each footprint distribution formally extends beyond any finite target area. Therefore, in those footprint calculations that involve a surface property distribution such as the LCC map, we normalize the footprint integrated over the map area to 1, unless indicated otherwise. This means that the upper distance of radial integration in Eqs. (28)–(440) is set to a finite limit of r_m and the footprint-weighted averages are scaled by dividing by $\int_0^{r_m} \int_0^{2\pi} f(\theta, r) d\theta dr$, where r_m (≈ 1.4 km) is the radius of the present [land coversurface](#) maps.

2.2.43 Examples of flow conditions

To demonstrate how the EC flux measurement at Tiksi is affected by surface heterogeneity, we calculated ~~with Eq. (8)~~ the footprint-weighted averages of the surface attributes LAI, terrain elevation and TWI [using Eq. \(2\) and the data illustrated in Figs. 1b–d as the continuous variable X, and with while](#) Eq. (440) [was used for](#) the footprint-weighted LCC areas of the nine classes shown in Fig. 1a. For this demonstration, we defined three flow situations in terms of the variables that affect the footprint in a given θ , i.e., U , u_* , L^{-1} and σ_v (Table 24). These cases represent differing stability conditions, for which typical parameter combinations were derived from the measurement data employed in this study. The $U - u_* - L^{-1}$ combination was constrained by $z_0 = 0.01$ m as calculated from the MOS profile of the horizontal wind speed (Pasquill and Smith, 1983). For lateral wind velocity fluctuations, we used the scaling $\sigma_v/u_* = 2.3$, which corresponds to the median of our data; for simplicity, this was adopted here for all stabilities.

2.3 Statistical model

2.3.1 Model formulation [and validation](#)

30 Assuming that the CH_4 flux does not vary among the LCC-map pixels attributed to a certain LCC, we applied Eq. (440) and expressed each flux measurement as a weighted arithmetic mean of the LCC-specific fluxes F_j , $j = 1 \dots N$ (number of LCCs),

$$\langle F \rangle = \sum_{j=1}^N \langle \Lambda \rangle_j F_j, \quad (642)$$

where these fluxes are unknown, and the weights $\langle \Lambda \rangle_j$ (Eq. 39) are the fractional areas of the corresponding LCCs. Assuming further that the LCC-specific fluxes remain constant within a data set of M (= 911 [in the full data set](#)) observations but the proportional LCC areas vary with the temporally changing footprint, we obtained a set of linear algebraic equations, from which a solution could be sought for F_j . We applied this idea by first defining aggregated LCC groups [according to the expected CH₄ source/sink capacity of each LCC, which procedure is detailed in Sect. 2.3.2](#), and formulated a linear regression problem as

$$\mathbf{A}\mathbf{q} = \mathbf{m} + \mathbf{e}, \quad (743)$$

where the matrix \mathbf{A} [$M \times (N_A + 1)$]- consists of the proportional LCC areas of the aggregated LCCs for each observation, \mathbf{q} [$(N_A + 1) \times 1$] is a vector of the unknown parameters, \mathbf{m} [$M \times 1$] denotes the measurement vector, and \mathbf{e} [$M \times 1$] is the error term. N_A ([= 3 here](#)) denotes the number of those aggregated LCCs whose proportional area was included as an explanatory variable. This does not cover all the LCCs, and we included an intercept term in this regression equation so as to represent the remaining LCCs and the proportion of footprint extending beyond the study area; i.e., we did not scale the sum of $\langle \Lambda \rangle_j$ to 100 %.

We estimated \mathbf{q} with the ordinary least square (OLS) estimator. Before calculating the standard errors of these estimates, we tested the model residuals for heteroskedasticity and serial correlation. Heteroskedasticity was tested with the White test that is based on an auxiliary regression, where squared residuals are regressed on original explanatory variables and their squares and cross products, and the inference is based on a Lagrange multiplier (LM) test statistic (Greene, 2012). Serial correlation was tested with the Breusch–Godfrey test, which is based on a similar LM principle where the OLS residuals are regressed on the original explanatory variables augmented by lagged residuals. If heteroskedasticity and serial correlation could not be ruled out, the standard errors for the model parameters were calculated with the Newey–West estimator, which is a robust estimator for the asymptotic covariance matrix of the OLS estimator (Greene, 2012). This would result in wider confidence intervals than the traditional OLS-based standard errors. We assume that these [confidence interval estimates](#) reflect the overall uncertainty emerging from measurement data, LCC classification and footprint modelling; [therefore no “bottom-up” error analysis addressing individual error sources was attempted](#).

The agreement between the model and the observations was evaluated on the basis of the coefficient of determination, (R^2), root mean squared error, (RMSE), and mean absolute error, (MAE). The agreement was also examined as a function of wind direction, to verify that we can replicate the pronounced directional dependency of the observed fluxes (Aurela et al., 2015). The performance of the statistical model against independent data was assessed with 10-fold cross-validation (James et al.,

2013). Assuming that model residuals represent the maximum measurement error, a conservative estimate for the random error of the measured mean flux was estimated as $RMSE/\sqrt{M}$.

2.3.2 Land cover class aggregation and upscaling of CH₄ fluxes

We hypothesize that mean CH₄ fluxes can be determined for LCC groups, ~~that are each~~ composed of LCCs of similar ~~according to their~~ expected source/sink capacity. This grouping was based on the documented vegetation and soil characteristics, reported in detail by Mikola et al. (2018) and Nyman (2015), and summarized here in Sect. 2.1.4. ~~There are also data available from a limited set of flux measurements made with static chambers in summer 2014 that provide guidance for the LCC grouping (Vähä, 2016).~~ In addition, we utilized the TWI map and defined areas of potentially wet soils as those with TWI > 4 (Fig. 1d). Using these data and syntheses of CH₄ production and fluxes in similar ecosystems (Olefeldt et al., 2013; Nicolini et al., 2013; Turetsky et al., 2014; Lau et al., 2015; Petrescu et al., 2015; Treat et al., 2015) as background information, we defined four aggregated classes (Table 32, Fig. 2), for which the LCC group-specific fluxes were determined with the statistical model described in Sect. 2.3.1.

The data sources listed above suggest that wet fens typically are strong CH₄ emitters, and thus the pixels of the wet fen LCC with TWI > 4 were selected for the first LCC group (“Strong source”). We also assumed that the pixels of the graminoid tundra LCC in the potentially wet locations should be included in this category as the graminoids at the site are dominated by aerenchymatous *Carex* spp. and *Eriophorum* spp. (e.g., *E. vaginatum*) (Nyman, 2015), i.e., plants known to be associated with substantial CH₄ emissions. Other fens likely act as weaker emitters, so these ~~were~~ combined into another LCC group (“Moderate source”), together with the bodies of freshwater (water LCC above the sea level). The previous data also justify an assumption that mineral soils, i.e., here the bare ground and lichen tundra LCCs, act as weak CH₄ sinks (“Sink”). The proportional areas of these three LCC groups were used as the explanatory variables in the regression model (Eq. 743), ~~i.e., $N_A = 3$.~~ The remaining pixels were allocated to the fourth group consisting of the LCCs that either are expected to have a very small CH₄ flux on average or cover only a limited area in flux footprints (“Neutral”). This group is included as an intercept in the regression model, and we hypothesize that its estimated value is not statistically different from zero.

The CH₄ fluxes determined for the aggregated LCCs defined above were upscaled by a simple mosaic approach, i.e., by areal weighting of the group-specific fluxes. To illustrate how the upscaled flux depends on ~~land cover surface~~ heterogeneity at different spatial scales, the upscaling was performed for different sub-domains as a function of the distance from the EC tower, and also for a larger area of 35.8 km² (Fig. S24 in the Supplement).

To investigate the temporal trend of the fluxes, we performed the statistical modelling and upscaling separately for weekly periods in addition to the full eight-week data set. These results also shed light on the performance of the statistical method when the number of input data is limited and the coverage of different wind direction may be incomplete.

3 Results and discussion

3.1 Demonstrating surface heterogeneity

To illustrate the expected range of flux footprint distributions of the EC measurements at Tiksi, Table 3 presents characteristic source area dimensions calculated with the meteorological data detailed in Table 1. Different source area definitions introduced in Sect. 2.2.1 are included: a full three dimensional footprint, Π (Eq. 3), for a single, arbitrary wind direction; the corresponding cross wind integrated footprint, Π_C (Eq. 7); and an annular footprint climatology, Π^* (Eq. 4), calculated assuming an equal frequency of wind directions (in which case Π^* equals Π).

Table 3 demonstrates expected qualitative features of flux footprints: the source areas are extensive over the aerodynamically smooth tundra terrain, and their dimensions increase with increasing atmospheric stability and with the proportional contribution to the measured flux, P (Schmid, 1994). While the distance of maximal surface influence in a single footprint varies by a factor of 2 ($r_{\max} = 18\text{--}35\text{ m}$), depending on stability, for the estimated far end of the source area contributing 90 % to the flux this factor is almost 20 ($r_{p,z} = 200\text{--}3500\text{ m}$). For the annular climatology, the dimensions are somewhat smaller (Table 3). It is noteworthy that variation in the efficiency of horizontal diffusion also plays a marked role in the spatial weighting of different surface elements and that the results for the cross wind integrated footprint are not identical to those for the three dimensional function; however, they are similar to the dimensions of the annular climatology. If the integration for the climatology case originated from the EC tower (Π_0 and Π_0^*), the resulting distance would be very close to $r_{p,z}$ (results not shown). Overall, these results indicate that, when reporting dimensions of the area of influence, it is important to state the definition adopted for this source area.

Our footprint analysis shows that those surface elements that had the greatest influence on the EC measurements at Tiksi were typically located within a distance of 10–200 m (Table S1 in the Supplement). However, the actual range depended strongly on atmospheric stability, as expected (Horst and Weil, 1992). The distance of maximal influence in a single footprint varied from 18 to 35 m depending on stability, and the estimated far end of the source area ranged from 200 to 3500 m for the 90 % flux contribution, for instance. The 1.4 km radius of the circle centred at the EC tower, which defines our primary study area, was selected to result in a 95 % footprint coverage within this area in the neutral case. About 15 % of the footprint calculated for the stable flow example extended beyond the limits of this area, while in the unstable case 99.7 % of the footprint was confined to the target circle (Fig. 3).

-The variation of the footprint-weighted LCC contributions, calculated with Eq. (410), as a function of wind direction demonstrates how the ~~surface~~ heterogeneity inherent in tundra landscape manifests itself in the EC measurement data (Fig. 3; see also Fig. S32 in the Supplement). As is obvious from the LCC map (Fig. 1a), ~~there are large differences in~~ the distribution of ~~the~~ contributing LCCs varied a lot among different wind directions (Fig. 3). In the neutral case, for example, there ~~were~~ seven different LCCs dominating at least in one sector. Turbulent mixing also played a substantial role in the magnitude of relative LCC contributions, as the weighting of longer distances increases with increasing stability. In some directions, the contribution of the most common LCCs was highly sensitive to atmospheric stability. In the north-east-to-east sector, for example, the ~~rather limited~~ relatively small dry fen patch located within a few tens of metres from the EC tower (Fig. 1a) contributed 45 % in the unstable case, ~~while its contribution is~~ but only 13 % in the stable case (Fig. 3). Similarly, the relative importance of the extensive bare-ground area between the west and the north-east strongly depended on atmospheric stability.

The footprint-weighted surface characteristics, calculated with Eq. (28) for the cases detailed in Table 42, further demonstrate the landscape heterogeneity-induced variations. The effective LAI originating from the footprint-weighting of the LAI map shows a strong dependency on wind direction: in the neutral case, for example, $\langle \text{LAI} \rangle$ ranges from 0.19 to 0.64 $\text{m}^2 \text{m}^{-2}$ (Fig. 4a). In the unstable case, the direction dependency was similar; however, ~~the~~ $\langle \text{LAI} \rangle$ ~~values are~~ was up to 0.12 $\text{m}^2 \text{m}^{-2}$ lower than in neutral conditions due to the dominance of bare ground in the vicinity of the EC tower in the north-western sector (Fig. 1a). As averaged over all directions, here assumed equally frequent, $\langle \text{LAI} \rangle$ was in all stability cases somewhat higher than the arithmetic areal average (Fig. 4a). Due to the directional variations in $\langle \text{LAI} \rangle$, the maximum sensor location bias (Δ_{LAI} , Eq. 54) may exceed 90 % in the direction of the maximum $\langle \text{LAI} \rangle$ (Fig. 4d).

Based on a corresponding footprint-weighting, an effective mean value could also be determined for terrain elevation (Fig. 4b). This shows that, even though the topographic variability within the flux footprint was ~~small~~ is limited, slightly different terrain elevation patterns are associated with each flux measurement depending on both wind direction and stability. The sensor location bias for elevation was negative in almost all flow conditions, as the elevation is on average lower within the area that typically dominates the flux footprint (Figs. 1b and 4b). The area of predominantly bare ground was also apparent in the effective TWI (Fig. 4c). In the east-to-south sector, the differences between the stability classes are due to the higher TWI values determined along the coast (Fig. 1d) that gain in importance in stable conditions. Between the south-west and the north-west, in contrast, $\langle \text{TWI} \rangle$ was higher in unstable conditions, which results from the more pronounced influence of the brook running nearby the EC tower. The footprint-weighted TWI averaged over all directions was, in all cases, close to the arithmetic area average (Fig. 4e), with the magnitude of the corresponding sensor location bias being lower than 30 % (Fig. 4f).

In addition to the examples presented above, we demonstrate ~~the surface~~ heterogeneity of the Tiksi landscape by calculating the mean LAI and LCC contributions from the time series of EC measurements adopted for the present analysis. Fig. 1a shows the footprint climatology for the growing season 2014, depicted as the ~~smallest bounded region containing the surface elements that contribute to EC measurements by a certain fraction (Eq. S1 in the Supplement) cumulative flux according to the definition of Eq. (3) (only the further distance visible)~~. This source area is clearly asymmetric, and comparison with the data in Table ~~S1 (in the Supplement)~~ indicates that the source area ~~for a certain P~~ is more limited than the corresponding area in typical neutral conditions; i.e., it effectively reflects slightly unstable conditions. Weighting the LAI distribution by the mean footprint results ~~eds~~ in a bias of $\Delta_{\text{LAI}} = 20.2\%$. ~~For comparison, T~~ this is much larger than the bias in the normalized vegetation difference index (NDVI) estimated for EC sites in northern China: at the 1 km² scale, this bias ranged from -6.9 to 4.2 % at eight sites with low vegetation, and even at a land model scale of ~300 km² the mean absolute bias was not more than 6.5 % (Wang et al., 2016). Notwithstanding such a high degree of agreement, one of the sites was considered “disturbed”. ~~In another study, Kim et al. (2006) estimated the EC measurements at two sites with an NDVI sensor location bias of less than 4 % for both an oak/grass and a slash pine site at the 1 km² scale and concluded that the related EC measurements were considered unbiased, while a bias of 28 % determined for a grassland site was judged aseonsidered~~ problematic (Kim et al., 2006).

For most of the LCCs at Tiksi, the field of view of the EC sensors averaged over the growing season clearly differ ~~eds~~ from the areal coverage of the LCCs within the study area (Table 4; see also Fig. ~~S43 (in the Supplement)~~ for the effect of wind direction and stability). ~~Here we have excluded the large marine areas, which have a minor weight in the EC data.~~ The difference is ~~still~~ largest for the water LCC, ~~as the freshwater bodies pixels of which~~ are concentrated on the fringes of the study area, and for the flood meadow category with a limited coverage. ~~, but~~ However, there ~~were~~ are also major differences among the dominating terrestrial classes, such as shrub tundra and wet fen; the surface elements attributed to these LCCs contributed ~~d~~ to the EC observations less (by ~~37-40~~ %) than their total areal coverage would suggest. ~~Rescaling the proportions after removing the marine water pixels from the study area for their limited footprint weight further amplifies this difference.~~

If the areal LCC proportions ~~were~~ are calculated within the non-circular area defined by the 90 % cumulative footprint (Eq. 3; Fig. 1a), some of these proportions changed ~~d~~ dramatically (Table 4). We also included in the comparison the LCC distributions ~~for a circle with a radius of 1 km, which halves the study area, and~~ for a 35.8 km² area (Fig. ~~S21~~ in the Supplement). Compared to ~~this the latter~~, the study area has a similar coverage of fens, bare ground and lichen tundra, ~~whereas; the~~ water and shrub tundra ~~LCCs~~ surfaces are under-represented, and bogs and graminoid tundra ~~are~~ over-represented. Overall, these results demonstrate the multiscale heterogeneity of the site and indicate that here the representativeness cannot be described as a proportional coverage of a single target LCC in the footprint climatology, as is the case for most EC sites (Göckede et al., 2008).

3.2 Land cover group-specific fluxes

The parameters of the regression model introduced in Sect. 2.3.1 were estimated with OLS for the LCC aggregation presented in Sect. 2.3.2. ~~FAs~~ this produced model residuals that exhibited both heteroscedasticity and autocorrelation (White LM test statistic $MR^2 = 92 > \chi_{0.99(9)}^2$, Breusch–Godfrey LM test statistic $(M - 1)R^2 = 117 > \chi_{0.99(1)}^2$). ~~Thus~~ the confidence intervals were based on the ~~heteroskedasticity and autocorrelation consistent~~ Newey–West estimator. Even when these (larger) confidence intervals were introduced, all the estimated parameters except for the constant, i.e., those representing aggregated LCCs with expected CH₄ exchange, proved to be statistically different from zero ($p < 0.05$; Table 5). The results were also in perfect accord with our qualitative hypothesis on CH₄ flux variability among the LCCs: the model could differentiate between the high emitters, moderate emitters and sinks without any explicit prior information on this pattern. Concerning the quantitative differences, Treat et al. (2018) reported the same degree of spatial variation (standard deviation/mean = 155 %) in the modelled annual CH₄ fluxes on low Arctic tundra, highly heterogeneous similarly to Tiksi, and showed that the differences among LCCs clearly dominate over the interannual variation in the regional CH₄ fluxes.

The temporal variation of the estimated 30 min ecosystem-scale CH₄ fluxes ~~was~~ consistent with observations, even though it is obvious that the full range of variability, most notably the peak values, ~~can~~ could not be reproduced ($R^2 = 0.797$, RMSE = 0.0994 $\mu\text{g CH}_4 \text{ m}^{-2} \text{ s}^{-1}$, MAE = 0.0686 $\mu\text{g CH}_4 \text{ m}^{-2} \text{ s}^{-1}$). However, part of this variation ~~arose~~ arises from measurement noise, and in this context it is crucial that the mean fluxes ~~were~~ are modelled accurately also when considering the strong wind direction dependence of observations (Fig. 5). Estimated from the binned mean fluxes shown in Fig. 5, the variance related to wind direction accounted for up to 80 % of the total variance of measured fluxes. This dependence, obviously generated by the systematic LCC variations within the flux footprint (Fig. 3), is a key pattern in this data set and must be taken into consideration when calculating representative CH₄ balances (Aurela et al., 2015). The model residuals differed significantly ($p < 0.05$) from zero only in a narrow southeastern wind sector, where the model slightly overestimated ~~s~~ the fluxes. The 10-fold cross-validation statistics show that the model performed ~~s~~ against independent data only marginally worse than the fit to the full data set ($R^2 = 0.794$, RMSE = 0.1000 $\mu\text{g CH}_4 \text{ m}^{-2} \text{ s}^{-1}$, MAE = 0.0691 $\mu\text{g CH}_4 \text{ m}^{-2} \text{ s}^{-1}$).

Forbrich et al. (2011) have shown that the footprint variations dominate the short-term (hourly to daily) variations in the CH₄ flux on a boreal fen with a pronounced flark–lawn–hummock structure, while soil temperature only explains the seasonal trend. As 80 % of the CH₄ flux variance at Tiksi was explained by the variation in the proportions of the LCCs contributing to the measurement, we can expect a similar pattern, i.e., a limited role of other environmental controls in the short-term variability (30 min data). The correlation between CH₄ flux and soil temperature (at 10 cm depth) was indeed weak ($R^2 = 0.101$) and did not get any stronger if one considered the model residual, i.e. the unexplained part of observation. For u_* , this

correlation was even weaker ($R^2 = 0.053$); u_* acts as a measure of turbulence that affects surface diffusion and ebullition and has been found to explain a major part of the CH_4 flux variance observed on polygonal tundra (Sachs et al., 2008). Our results also contrasted with the findings of Parmentier et al. (2011) who, similarly to our study, observed a major effect of wind direction on the CH_4 flux measured on Siberian tundra but were also able to relate the short-term flux variation to environmental variables, including atmospheric stability. In that study, however, the LCC proportions were not used as an explanatory factor, but the data were grouped according to the wind sector characterized by qualitative soil wetness (“wet”, “dry” and “mixed”), and environmental responses were determined separately for these groups. On the other hand, Tagesson et al. (2012) found that the only significant factor controlling the CH_4 flux on a wet tundra ecosystem in north-east Greenland was the relative contribution of fen areas, indicating that the controls are site-specific and that any turbulence-related dependency may partly reflect footprint variations, in addition to the actual control of surface exchange processes.

Chamber-based CH_4 flux measurements would constitute the most logical means for validating the estimated LCC-specific fluxes. As explained in Sect. 2.1.2, some chamber data were available for the period of the EC data but their temporal and spatial coverage were limited. Despite the limitations, these measurements lent support to our EC-based results: the two wet fen plots were strong CH_4 emitters with observed fluxes of 0.56 and 3.8 $\mu\text{g CH}_4 \text{ m}^{-2} \text{ s}^{-1}$, while the mean CH_4 emission from dry fen plots ranged from 0.06 to 0.67 $\mu\text{g CH}_4 \text{ m}^{-2} \text{ s}^{-1}$ (mean 0.25 $\mu\text{g CH}_4 \text{ m}^{-2} \text{ s}^{-1}$) (Vähä, 2016). The LCC group-specific fluxes ~~are~~ were also in accordance with the extensive synthesis of chamber-based CH_4 flux measurements across permafrost zones conducted by Olefeldt et al. (2013). ~~This~~ Their database indicates that the mean flux at peatland sites during the growing season ranges from 0.03 $\mu\text{g CH}_4 \text{ m}^{-2} \text{ s}^{-1}$ on dry tundra to 0.75 $\mu\text{g CH}_4 \text{ m}^{-2} \text{ s}^{-1}$ on wet tundra (medians of site-specific fluxes), while the mean flux at the sites classified as permafrost fen ~~is~~ was within 0.48–1.70 $\mu\text{g CH}_4 \text{ m}^{-2} \text{ s}^{-1}$ at 50 % of the sites. The micrometeorological measurements that integrate over the ~~surface~~ heterogeneity of tundra landscape typically show lower CH_4 fluxes. For example, Sachs et al. (2008) and Wille et al. (2008) measured a mean CH_4 emission of 0.22 $\mu\text{g CH}_4 \text{ m}^{-2} \text{ s}^{-1}$ from polygonal tundra in the ~~nearby~~ Lena River delta in July–August (in 2004 and 2006), which is close to our mean flux (0.21 $\mu\text{g CH}_4 \text{ m}^{-2} \text{ s}^{-1}$ in July–August 2014). ~~Seven~~ Eight other comparable Arctic tundra sites in Siberia, Alaska and Greenland had a mean summer flux within the range of 0.13–1.05 $\mu\text{g CH}_4 \text{ m}^{-2} \text{ s}^{-1}$ (Fan et al., 1992; Friborg et al., 2000; Zona et al., 2009; Parmentier et al., 2011; Tagesson et al., 2012; Castro-Morales et al., 2018). These data also show that variation among sites can be much larger than the interannual variation at a site.

The sink efficiency estimated for the mineral soil LCCs at Tiksi ($-0.131 \pm 0.042 \mu\text{g CH}_4 \text{ m}^{-2} \text{ s}^{-1}$, 95 % confidence interval) seems high in comparison when compared to previous data (Turetsky et al., 2014; Lau et al., 2015; Jørgensen et al., 2015; D’Imperio et al., 2017). However, this estimate is consistent with the measured EC fluxes and thus not an artefact of the modelling procedure. This can be observed by inspecting the cases in which the proportion of the assumed sink LCCs in the flux footprint exceeds 80 % (within the wind direction sector of 330–360°). By ignoring the other LCCs, we obtained an apparent mean CH_4 flux of $-0.109 \mu\text{g CH}_4 \text{ m}^{-2} \text{ s}^{-1}$ for these cases, while the corresponding modelled (for all LCCs) and

measured fluxes ~~were~~ ~~are~~ -0.093 and -0.094 $\mu\text{g CH}_4\text{ m}^{-2}\text{ s}^{-1}$, respectively. Furthermore, ~~the~~³² chamber measurements ~~were~~ conducted on bare ground at the site in summer 2014, yielding ~~ed~~ ~~ing~~ a consistent mean of -0.12 $\mu\text{g CH}_4\text{ m}^{-2}\text{ s}^{-1}$ (Vähä, 2016).

5 So far, our discussion has been based on fluxes averaged over the whole study period of eight weeks. The weekly resolved LCC group-specific fluxes, however, indicate that there was temporal variation in CH₄ emissions that was not generated by footprint dynamics (Fig. 6). Most notably, the drier fens (dry fen LCC, and wet fen LCC with a low TWI) showed only weak emissions in the beginning of the period. The maximum emissions occurred during the two-week period around mid-August (9–22 August); these emissions were on average 0.44 ± 0.14 $\mu\text{g CH}_4\text{ m}^{-2}\text{ s}^{-1}$ for the “Moderate source” LCC group and $1.00 \pm$
10 0.10 $\mu\text{g CH}_4\text{ m}^{-2}\text{ s}^{-1}$ for the “Strong source” LCC group. The weekly averages of model residuals during the whole study period were positively correlated with the corresponding soil temperatures, but the correlation was not statistically significant ($R^2 = 0.444$, $p = 0.102$). However, the maximum emissions occurred when soil temperatures were highest, ca. 5
15 °C (at 10 cm depth), in 9–22 August. During this period, the LAI of vascular plants on the fens and graminoid tundra was still high, even though already declining on the fens (Juutinen et al., 2017). The positive correlation between the vascular LAI of graminoid tundra and the weekly model residuals ($R^2 = 0.556$, $p = 0.054$) points to the role of both primary production and plant-mediated CH₄ transport, associated with the close relationship between LAI and the maximum photosynthesis rate (Laurila et al., 2001; Street et al., 2007) and the dominance of aerenchymatous plants (Bridgham et al., 2013). However, the depth of the active layer also increased during the study period in some soils, especially in dry fens, but the data are too limited for statistical analysis of this effect (Mikola et al., 2018).

20 ~~Our results are necessarily influenced by the quality of the land cover classification. The accuracy assessment indicates that especially the flood meadow LCC is poorly classified (Mikola et al., 2018); however, this LCC only appears along the brook and has a very limited coverage. More importantly, the dry fen, wet fen and graminoid tundra pixels may be partly mixed up. The field data and multivariate data analysis of Mikola et al. (2018) indicate that the variation in plant functional type composition within these LCCs indeed overlap, which impairs the separation between the strong and moderate source LCC groups. On the other hand, the large areas of bare ground and lichen tundra with low organic soil content, i.e., the assumed CH₄ sink areas, could be identified reliably (Mikola et al., 2018). Despite the uncertainties, the classification of vegetation types allows us to meaningfully group the surface elements also according to their CH₄ exchange potential. This relationship shows that vegetation type reflects the integrated effect of a range of processes that control net production and efflux of CH₄, such as the availability of substrates and gas transport routes (Davidson et al., 2016, 2017). Thus a vegetation classification based on VHSR satellite imagery provides us with a straightforward means of upscaling the average LCC specific fluxes without considering environmental controls.~~

25
30

3.3 Upscaled CH₄ fluxes

By upscaling the mean CH₄ fluxes estimated for the LCC groups, we estimated the effect of ~~the~~ EC tower location on the spatial representativeness ~~offer~~ the mean CH₄ flux observed during the growing season of 2014 ($0.208 \mu\text{g CH}_4 \text{ m}^{-2} \text{ s}^{-1}$). In other words, adopting the data shown in Table 5 as a reference for the CH₄ flux averaged over the study area, we could calculate the sensor location bias for CH₄ flux (Fig. 5) similarly to the results shown in Sect. 3.1 for LAI, terrain elevation, TWI and LCC proportions. As the relative area of the coastal waters is significant within the study area but minor in the average flux footprint (Fig. 1, Table 4), these ~~water~~ areas were excluded from the upscaling domain.

Calculating the sensor location bias for CH₄ flux equals to a linear transformation of the observed fluxes. Thus the pronounced directional dependence of CH₄ fluxes translates into an equally pronounced variation in this bias estimate, which ranges approximately from -200 to 400 % for individual data points and from -170 to 230 % on average (Fig. 5). The bias was smallest in eastern and western wind directions. However, the effective LCC composition is very different in these directions, with a much smaller coverage of fens in the west (Fig. 3).

The areally averaged CH₄ flux depends on the upscaling domain in a non-monotonous manner (Fig. 67). The uncertainty of the mean measured CH₄ flux, which was estimated from the model residuals (Sect. 2.3.1), was small ($0.007 \mu\text{g CH}_4 \text{ m}^{-2} \text{ s}^{-1}$) due to a large number of observations and was ignored in Fig. 7b. Defining the reference area as a function of the radius of a circular area centred at the EC tower, the magnitude of sensor location bias is less than 30 % for the distances exceeding 80 m, and was less than 10 % for the distances of ca. 640–1350 m. Acknowledging the statistical uncertainty in the upscaled fluxes, determined from the LCC group-specific uncertainty estimates (Table 5), the measured mean flux was within the 95 % confidence interval for distances larger than ca. 600 m. For the primary study area, the mean bias during the growing season was 13.9 % and the corresponding 95 % confidence interval was [-0.3 %, 32.9 %] (Table 6).

While formally the overestimation of EC measurements of the CH₄ flux averaged over the study area was not statistically significant ($p > 0.05$), the estimated sensor location bias could be minimized by reducing the radius to would be lower if the study area were originally defined by a radius of 800–1000 m. Here we do not suggest that the study area should be defined post hoc but advocate a footprint-based analysis to assess the representativeness of measurements at different spatial scales. Adopting the regional upscaling area of 35.8 km^2 as the reference for results in a sensor bias of 30 % [12 %, 55 %] for the CH₄ flux (Table 6). Considering the CH₄ fluxes alone, the LCC distribution shown for the area extending to 1 km from the EC tower would be a suitable choice for a representative site description.

Even though the coverage of ~~the-our~~ nine basic LCCs clearly differs from their footprint-weighted contributions (Table 4), the four LCC group classes aggregated according to their assumed CH₄ emission potential of LCCs covered areas rather

similar to those within the original study domain (Table 6). Within the regional upscaling area of 35.8 km², the strong emitters ~~were~~are less common, but the total flux ~~was~~is only 13 % lower than within the original study area. On the other hand, freshwater bodies occupy a larger relative area (Table 4). These were included here in the “~~M~~moderate source” LCC group, but the actual emissions from these ~~ecosystems~~surfaces could not be estimated as their total area within the flux footprint is minute. Nevertheless, there is ~~an increasing amount of~~ evidence that Arctic lakes and ponds ~~may~~emit significant amounts of CH₄ (Wik et al., 2016). At all scales, it ~~was~~is necessary to allow for the sink areas that play a significant role in the upscaled balance. However, the agreement of CH₄ fluxes between different scales may be considered somewhat fortuitous and implies little about carbon dioxide and other scalar fluxes that have different spatial patterns. ~~For example, Chen et al. (2009) estimated a sensor location bias of up to 55 % for the monthly gross primary production of a Douglas fir-dominated forest.~~

3.4 Methodological issues

~~Our results obviously depend on the quality of the land cover classification. The LCC accuracy assessment indicates that especially the flood meadow LCC is poorly classified (Mikola et al., 2018); however, this LCC only appears along the brook and has a very limited coverage. More importantly, the dry fen, wet fen and graminoid tundra pixels may be partly mixed up. The field data and multivariate data analysis of Mikola et al. (2018) indicate that the variation in plant functional type composition within these LCCs indeed overlap, which impairs the classification of the “Strong source” and “Moderate source” LCC groups and effectively precludes modelling that resolves individual LCCs. On the other hand, the large areas of bare ground and lichen tundra with low organic soil content, i.e., the assumed CH₄ sink areas, can be identified reliably (Mikola et al., 2018).~~

~~Despite the uncertainties, the land cover classification allowed us to meaningfully group the surface elements according to their CH₄ exchange potential. This relationship shows that the LCC reflects the integrated effect of a range of processes that control net production and efflux of CH₄, such as the availability of substrates and gas transport routes (Davidson et al., 2016, 2017). Thus a vegetation classification based on VHRS satellite imagery provided us with a straightforward means of upscaling the average LCC group-specific fluxes. As the predominant part of CH₄ flux variance resulted from the varying contributions of different LCCs, we did not consider additional environmental controls. Such simplicity is welcome since statistically robust EC-based flux estimates for scales exceeding the flux footprint would require spatial replication with multiple EC towers (Hill et al., 2017). Our approach serves as an alternative to a common method of deriving LCC-specific data from (a typically more limited set of) flux chamber measurements and upscaling these either directly (e.g., Schneider et al., 2009; Davidson et al., 2017) or by first modelling their temporal variation (e.g., Marushchak et al., 2016). Matthes et al. (2014) showed that more nuanced insights into the spatial drivers can be achieved by the use of multiple EC towers and periodic remote sensing images and by examination of both the abundance and spatial fractal structure of vegetation.~~

Even though the KM model constitutes an appropriate tool for describing turbulent transport over an aerodynamically smooth surface such as tundra, any footprint estimate involves both structural and input-related modelling uncertainties. The KM model has been tested by Kljun et al. (2003), Marcolla and Cescatti (2005), Neftel et al. (2008) and Arriga et al. (2017) against experimental data and more complex footprint models. All these studies conclude that the KM model performs well, but we note here that there may be a tendency for too smooth footprint distributions in the along-wind direction. As pointed out in Sect. 2.3.1, we did not try to explicitly estimate the errors related to the flux footprints but assumed that the confidence intervals determined for the LCC group-specific fluxes reflect the overall uncertainty contained in any data employed in the statistical model. Because of this approach, the uncertainty of the results shown in Figs. 3 and 4 could not be quantified. Overestimation of footprint distribution in larger distances would mean that the contribution of graminoid tundra might be slightly underestimated and that of shrub tundra overestimated as the proportions of these LCCs have a rather systematic dependency on the distance from the EC mast. If the overall LCC heterogeneity of a site became more apparent when viewing it as a function of distance rather than direction, our statistical method would be more dependent on the footprint model and the results would probably be more uncertain.

We obtained statistically significant estimates for the LCC group-specific fluxes when employing the whole data set of eight weeks, but the performance of the model was observed to deteriorate as the number of data was reduced. This can be observed from the weekly results (Fig. 6), in which the confidence intervals are temporally varying and larger than those for the whole data set; in some cases, the results were not consistent with the original flux hypotheses (at the chosen significance level). As wind direction is the primary control of the flux footprint, and consequently the LCC proportions associated with EC measurements (Fig. 3), it is necessary that the variation in wind directions during each period sufficiently covers all the relevant LCCs. This obviously depends on the degree and nature of LCC heterogeneity at the site in question. In our weekly results for Tiksi, the directional coverage was clearly incomplete during 16–22 August, when there were few observations for the sector extending from the north-west to the south-east, leading to uncertain flux estimates for that particular period (Fig. 6).

While the weekly results indicated that there is temporal variation in the LCC group-specific fluxes, the longer-term upscaling was rather insensitive to temporal resolution of these data. The weekly values produced an upscaled flux of $0.162 \pm 0.063 \mu\text{g CH}_4 \text{ m}^{-2} \text{ s}^{-1}$ for the original study area, i.e., only slightly lower (by 11 %) but much more uncertain estimate than the one obtained for the whole data set (Table 6).

We suggest that estimation of LCC-specific fluxes, accomplished here with a regression model, provides a new avenue to filling the inevitable gaps in the measurement data time series. This proposition is supported by the good out-of-sample validation statistics obtained, as holding the validation data out during parameter estimation is equivalent to generating missing data that need to be gap-filled. This kind of an approach is potentially applicable to those data gaps that are related

to the gas concentration measurement, for example due to malfunctioning of the gas analyser, i.e., gaps that appear in the CH_4 flux data but not in the momentum and sensible heat fluxes.

Another methodological implication of our results concerns the definition of a study area. It is customary to report a “site description” that documents the key ecological characteristics of the area of interest. Within a homogeneous environment, collating the necessary site data is straightforward in terms of statistical representativeness because the outcome is insensitive to the spatial sampling design. Furthermore, the representativeness of EC measurements can be simply assessed by considering the coverage of a single target LCC within the flux footprints. In heterogeneous environments, however, there is a risk for a serious mismatch between the EC flux measurements and the site data, even in cases of an unbiased description of the study area. Our results show that the land cover type composition sampled by the EC measurement was significantly different from the actual LCC coverage within our study area, which as such was originally chosen to be consistent with the dimensions of a typical flux footprint and considered characteristic of the landscape.

4 Conclusions

The eddy covariance flux measurement technique is commonly considered to have an advantageous spatial averaging property, sometimes to the extent that it is assumed to “provide an accurate integration of the overall flux from the [heterogeneous] ecosystem” (Turner and Chapin III, 2006). However, this notion is limited and potentially misleading as a universal premise, since this integration process involves differential-~~and temporally varying~~ weighting within a temporally varying flux footprint, a well-known but frequently overlooked feature of EC measurements, which we in the present study demonstrated and quantified for a heterogeneous tundra site in northeastern Russia. The CH_4 fluxes measured at Tiksi were highly variable due to the variation in vegetation composition and soil wetness within the ~~tundra~~ landscape around the EC tower. During summer 2014, the ~~mean~~-bias of observations with respect to the upscaled flux varied strongly with wind direction, ranging from ~~-170200~~ to ~~230200~~ % on average.

By combining VHSR satellite imagery and footprint modelling, we could statistically estimate the contribution of the main land cover types to EC measurements. Methane emissions mainly originated from wet fen and graminoid tundra patches in locations with topography-enhanced soil wetness, where conditions are favourable for CH_4 production and efflux (mean flux ~~0.951.0~~ $\mu\text{g CH}_4 \text{ m}^{-2} \text{ s}^{-1}$ during the two-week peak period in summer 2014). Another noteworthy feature is that the areas of bare soil and lichen tundra acted as strong CH_4 sinks ($-0.13 \mu\text{g CH}_4 \text{ m}^{-2} \text{ s}^{-1}$ during the summer). Despite the ~~ecosystemsurface~~ heterogeneity and directional variations in the point-to-area representativeness of EC measurements, the mean CH_4 flux measured during this season can be considered unbiased, and even more so if the present area of interest ~~were~~is halved, i.e., considered to extend up to 1 km from the EC tower. On the other hand, the measured fluxes overestimate the regional (35.8 km^2) balance by 30 %.

5 An important implication emerging from our results concerns the definition of the study area. It is customary to report a “site description” that documents the key ecological characteristics of the area of interest. Within a homogeneous environment, collating the necessary site data is straightforward in terms of statistical representativeness because the outcome is insensitive to the spatial sampling design. Furthermore, the representativeness of EC measurements can be simply assessed by considering the coverage of a single target LCC within the flux footprints. In heterogeneous environments, however, there is a risk for a serious mismatch between the EC flux measurements and the site data, even in cases of an unbiased description of the study area. Our results show that the land cover type composition sampled by the EC measurement was significantly different from the actual LCC coverage within our study area, which as such was chosen to be consistent with the dimensions of a typical flux footprint and considered characteristic of the landscape. There were large differences in the weighting of the LCCs also when averaged over a full growing season. Thus the small scale heterogeneity was so high as to result in rather unfavourable representativeness metrics for key surface features such as LAI and LCC fractions, Even though the EC-sampled LCC distribution proved to be representative in terms of the mean CH₄ flux during a growing season, the small-scale heterogeneity at the site was so high as to result in rather unfavourable representativeness metrics for key land cover features such as LAI and LCC fractions. ~~These findings~~ This suggests that it would generally be beneficial to present a more integrated site and flux data description than what has been considered standard, i.e., to also include data on footprint-weighted surface attributes ~~data~~ and point-to-area representativeness.

20 In a follow-up study, we will investigate longer-term annual CH₄ flux data from Tiksi to better understand the seasonal and interannual variations and their environmental controls ~~and to derive long-term CH₄ balances.~~ These data will also make it possible to further assess the statistical method suggested here, including its use as a gap-filling tool. ~~We assume that estimation of LCC specific fluxes, accomplished here with a regression model, provides a new avenue to filling the inevitable gaps in the measurement data time series. This proposition is supported by the good out of sample validation statistics presented, as holding the validation data out during parameter estimation is equivalent to generating missing data that need to be gap filled. This kind of an approach is potentially applicable to those data gaps that are related to the gas concentration measurement, for example due to malfunctioning of the gas analyser, i.e., gaps that appear in the CH₄ flux data but not in the momentum and sensible heat fluxes.~~ Furthermore, we anticipate that flux sites with more than one EC tower provide new opportunities for the estimation of LCC-specific fluxes (e.g., Matthes et al., 2014; Hill et al., 2017); more advanced inverse modelling techniques should be explored for this.

Acknowledgements

This study was financially supported by the Academy of Finland, projects “Greenhouse gas, aerosol and albedo variations in the changing Arctic” (project no. 269095), “Carbon balance under changing processes of Arctic and subarctic cryosphere” (project no. 285630), “Constraining uncertainties in the permafrost-climate feedback” (project no. 291736) and “Carbon dynamics across Arctic landscape gradients: past, present and future” (project no. 296888); the European Commission, [FP7](#) project “Changing permafrost in the Arctic and its global effects in the 21st century (PAGE21, [project no. 282700](#))”; and the Nordic Council of Ministers, DEFROST Nordic Centre of Excellence within NordForsk.

References

- AARI: Archive of Tiksi standard meteorological observations (1932–2016), Russian Federal Service for Hydrometeorology and Environmental Monitoring, St Petersburg, Russia, http://www.aari.ru/resources/d0024/archive/description_e.html, last access: ~~7 March~~ 13 September, 2018.
- 5 Amiro, B. D.: Footprint climatologies for evapotranspiration in a boreal catchment, *Agr. Forest Meteorol.*, 90, 195–201, 1998.
- [Arriga, N., Rannik, Ü, Aubinet, M., Carrara, A., Vesala, T., and Papale, D.: Experimental validation of footprint models for eddy covariance CO₂ flux measurements above grassland by means of natural and artificial tracers, *Agr. Forest Meteorol.*, 242, 75–84, 2017.](#)
- 10 Asner, G. P., Scurlock, J. M. O., and Hicke, J. A.: Global synthesis of leaf area observations: implications for ecological and remote sensing studies, *Glob. Ecol. Biogeogr.*, 12, 191–205, 2003.
- Aubinet, M., Vesala, T., and Papale, D. (Eds.): *Eddy Covariance: A Practical Guide to Measurement and Data*, Springer Science+Business Media B.V., Dordrecht, 2012.
- Aurela, M., Lohila, A., Tuovinen, J.-P., Hatakka, J., Riutta, T., and Laurila, T.: Carbon dioxide exchange on a northern
15 boreal fen, *Boreal Environ. Res.*, 14, 699–710, 2009.
- Aurela, M., Laurila, T., Tuovinen, J.-P., Hatakka, J., Linkosalmi, M., Virtanen, T., Mikola, J., Asmi, E., Ivakhov, V., Kondratyev, V., Uttal, T., and Makshtas, A.: CH₄ and CO₂ exchange on permafrost tundra in Tiksi, Siberia, in: *Proceedings of the 1st Pan-Eurasian Experiment (PEEX) Conference and the 5th PEEX Meeting*, ed: Kulmala, M., Zilitinkevich, S., Lappalainen, H. K., Kyrö, E.-M., and Kontkanen, J., Report Series in Aerosol Science, 163, Helsinki, Finland, 60–62, 2015.
- 20 Böhner, J. and Selige, T.: Spatial prediction of soil attributes using terrain analysis and climate regionalisation, in *SAGA – Analysis and Modelling Applications*, ed: Böhner, J., McCloy, K. R., and Strobl, J., Göttinger Geographische Abhandlungen, 115, University of Göttingen, Germany, 13–28, 2006.
- Bridgham, S. D., Cadillo-Quiroz, H., Keller, J. K., and Zhuang, Q.: Methane emissions from wetlands: biogeochemical, microbial, and modeling perspectives from local to global scales, *Glob. Change Biol.*, 19, 1325–1346, 2013.
- 25 Budishchev, A., Mi, Y., van Huissteden, J., Beletti-Marchesini, L., Schaepman-Strup, G., Parmentier, F. J. W., Fratini, G., Gallagher, A., Maximov, T. C., and Dolman, A. J.: Evaluation of a plot-scale emission model using eddy covariance observations and footprint modelling, *Biogeosciences*, 11, 4651–4664, 2014.
- Castro-Morales, K., Kleinen, T., Kaiser, S., Zaehle, S., Kittler, F., Kwon, M. J., Beer, C., and Göckede, M.: Year-round simulated methane emissions from a permafrost ecosystem in Northeast Siberia, *Biogeosciences*, [15, 2691–2722, 2018.](#)
30 [Discuss., <https://doi.org/10.5194/bg-2017-310>, in review, 2017.](#)

- Chen, B., Black, T. A., Coops, N. C., Hilker, T., Trofymow, J. A., and Morgenstern, K.: Assessing tower flux footprint climatology and scaling between remotely sensed and eddy covariance measurements, *Bound.-Lay. Meteorol.*, 130, 137–167, 2009.
- ~~Cooper, M. D. A., Estop Aragonés, C., Fisher, J. P., Thierry, A., Garnett, M. H., Charman, D. J., Murton, J. B., Phoenix, G. K., Treharne, R., Kokelj, S. V., Wolfe, S. A., Lewkowitz, A. G., Williams, M., and Hartley, I. P.: Limited contribution of permafrost carbon to methane release from thawing peatlands, *Nat. Clim. Change*, 7, 507–513, 2017.~~
- Davidson, S. J., Sloan, V. L., Phoenix, G. K., Wagner, R., Fisher, J. P., Oechel, W. C., and Zona, D.: Vegetation type dominates the spatial variability in CH₄ emissions across multiple arctic tundra landscapes, *Ecosystems*, 19, 1116–1132, 2016.
- 10 Davidson, S. J., Santos, M. J., Sloan, V. L., Reuss-Schmidt, K., Phoenix, G. K., Oechel, W. C., and Zona, D.: Upscaling CH₄ fluxes using high-resolution imagery in Arctic tundra ecosystems, *Remote Sens.*, 9, 1227, 2017.
- D’Imperio, L., Nielsen, C. S., Westergaard-Nielsen, A., Michelsen, A., and Elberling, B.: Methane oxidation in contrasting soil types: responses to experimental warming with implication for landscape-integrated CH₄ budget, *Glob. Change Biol.*, 23, 966–976, 2017.
- ~~15 Dyer, A. J.: The adjustment of profiles and eddy fluxes, *Q. J. Roy. Meteor. Soc.*, 89, 276–280, 1963.~~
- Fan, S. M., Wofsy, S. C., Bakwin, P. S., Jacob, D. J., Anderson, S. M., Keabian, P. L., McManus, J. B., Kolb, C. E., and Fitzjarrald, D. R.: Micrometeorological measurements of CH₄ and CO₂ exchange between the atmosphere and subarctic tundra, *J. Geophys. Res.*, 97, 16627–16643, 1992.
- ~~20 Foken, T. and Wichura, B.: Tools for quality assessment of surface-based flux measurements, *Agr. Forest Meteorol.*, 78, 83–105, 1996.~~
- Forbrich, I., Kutzbach, L., Wille, C., Becker, T., Wu, J., and Wilmking, M.: Cross-evaluation of measurements of peatland methane emissions on microform and ecosystem scales using high-resolution landcover classification and source weight modelling, *Agr. Forest Meteorol.*, 151, 864–874, 2011.
- ~~25 Friborg, T., Christensen, T. R., Hansen, B. U., Nordstroem, C., and Soegaard, H.: Trace gas exchange in a high-arctic valley 2. Landscape CH₄ fluxes measured and model using eddy correlation data, *Global Biogeochem. Cy.*, 14, 715–723, 2000.~~
- ~~Gash, J. H. C.: A note on estimating the effect of a limited fetch on micrometeorological evaporation, *Bound.-Lay. Meteorol.*, 35, 409–413, 1986.~~
- Göckede, M., Markkanen, T., Hasager, C. B., and Foken, T.: Update of a footprint-based approach for the characterisation of complex measurement sites, *Bound.-Lay. Meteorol.*, 118, 635–655, 2006.

Göckede, M., Foken, T., Aubinet, M., Aurela, M., Banza, J., Bernhofer, C., Bonnefond, J. M., Brunet, Y., Carrara, A., Clement, R., Dellwik, E., Elbers, J., Eugster, W., Fuhrer, J., Granier, A., Grünwald, T., Heinesch, B., Janssens, I. A., Knohl, A., Koeble, R., Laurila, T., Longdoz, B., Manca, G., Marek, M., Markkanen, T., Mateus, J., Matteucci, G., Mauder, M., Migliavacca, M., Minerbi, S., Moncrieff, J., Montagnani, L., Moors, E., Ourcival, J.-M., Papale, D., Pereira, J., Pilegaard, K., Pita, G., Rambal, S., Rebmann, C., Rodrigues, A., Rotenberg, E., Sanz, M. J., Pedlak, P., Seufert, G., Siebicke, L., Soussana, J. F., Valentini, R., Vesala, T., Verbeeck, H., and Yakir, D.: Quality control of CarboEurope flux data – Part 1: Coupling footprint analyses with flux data quality assessment to evaluate sites in forest ecosystems, *Biogeosciences*, 5, 433–450, 2008.

Greene, W. H.: *Econometric Analysis*, 7th Ed., Pearson Education Ltd., Harlow, UK, 2012.

10 Heikkinen, J. E. P., Maljanen, M., Aurela, M., Hargreaves, K. J., and Martikainen, P. J.: Carbon dioxide and methane dynamics in a sub-Arctic peatland in northern Finland, *Polar Res.*, 21, 49–62, 2002.

~~Hugelius, G., Strauss, J., Zubrzycki, S., Harden, J. W., Schuur, E. A. G., Ping, C. L., Schirmer, L., Grosse, G., Michaelson, G. J., Koven, C. D., O'Donnell, J. A., Elberling, B., Mishra, U., Camill, P., Yu, Z., Palmtag, J., and Kuhry, P.: Estimated stocks of circumpolar permafrost carbon with quantified uncertainty ranges and identified data gaps, *Biogeosciences*, 11, 6573–6593, 2014.~~

15 ~~Hill, T., Chocholet, M., and Clement, R.: The case for increasing the statistical power of eddy covariance ecosystem studies: why, where and how? *Glob. Change Biol.*, 23, 2154–2165, 2017.~~

Horst, T. W. and Weil, J. C.: How far is far enough?: The fetch requirements for micrometeorological measurements of surface fluxes, *J. Atmos. Ocean Tech.*, 11, 1018–1025, 1994.

20 James, G., Witten, D., Hastie, T., and Tibshirani, R.: *An Introduction to Statistical Learning with Applications in R*, Springer Science+Business Media, Inc., New York, 2013.

Jørgensen, C. J., Lund Johansen, K. M., Westergaard-Nielsen, A., and Elberling, B.: Net regional methane sink in High Arctic soils of northeast Greenland, *Nat. Geosci.*, 8, 20–23, 2015.

Juutinen, S., Virtanen, T., Kondratyev, V., Laurila, T., Linkosalmi, M., Mikola, J., Nyman, J., Räsänen, A., Tuovinen, J.-P., and Aurela, M.: Spatial variation and seasonal dynamics of leaf-area index in the arctic tundra – implications for linking ground observations and satellite images, *Environ. Res. Lett.*, 12, 095002, 2017.

25 Kim, J., Guo, Q., Baldocchi, D. D., Leclerc, M. Y., Xu, L., and Schmid, H. P.: Upscaling fluxes from tower to landscape: Overlaying flux footprints on high-resolution (IKONOS) images of vegetation cover, *Agr. Forest Meteorol.*, 136, 132–146, 2006.

[Kljun, N., Kormann, R., Rotach, M. W., and Meixner, F. X.: Comparison of the Lagrangian footprint model LPDM-B with an analytical footprint model, Bound.-Lay. Meteorol., 106, 349–355, 2003.](#)

Kormann, R. and Meixner, F. X.: An analytical footprint model for non-neutral stratification, Bound.-Lay. Meteorol., 99, 207–224, 2001.

- 5 Lai, D. Y. F.: Methane dynamics in northern peatlands: A review, Pedosphere, 19, 409–421, 2009.

Lau, M. C. Y., Stackhouse, B. T., Layton, A. C., Chauhan, A., Vishnivetskaya, T. A., Chourey, K., Ronholm, J., Mykityczuk, N. C. S., Bennett, P. C., Lamarche-Gagnon, G., Burton, N., Pollard, W. H., Omelon, C. R., Medvigy, D. M., Hettich, R. L., Pffifner, S. M., Whyte, L. G., and Onstott, T. C.: An active atmospheric methane sink in high Arctic mineral cryosols, ISME J., 9, 1880–1891, 2015.

- 10 [Laurila, T., Soegaard, H., Lloyd, C. R., Aurela, M., Tuovinen, J.-P., and Nordstroem, C.: Seasonal variations of net CO₂ exchange in European Arctic ecosystems, Theor. Appl. Climatol., 70, 183–201, 2001.](#)

[Laurila, T., Tuovinen, J.-P., Lohila, A., Hatakka, J., Aurela, M., Thum, T., Pihlatie, M., Rinne, J., and Vesala, T.: Measuring methane emissions from a landfill using a cost-effective micrometeorological method, Geophys. Res. Lett., 32, L19808, 2005.](#)

- 15 Leclerc, M. Y. and Foken, T.: Footprints in Micrometeorology and Ecology, Springer-Verlag, Berlin, 2014.

Leclerc, M. Y. and Thurtell, G. W.: Footprint prediction of scalar fluxes using a Markovian analysis, Bound.-Lay. Meteorol., 52, 247–258, 1990.

Livingston, G. P. and Hutchinson, G. L.: Enclosure-based measurement of trace gas exchange: applications and sources of error, in: Biogenic Trace Gases: Measuring Emissions from Soil and Water, ed: Matson, P. A. and Harriss, R. C., Blackwell Science Ltd., Oxford, UK, 14–51, 1995.

- 20 [Marcolla, B. and Cescatti, A.: Experimental analysis of flux footprint in varying conditions in an alpine meadow, Agr. Forest Meteorol., 135, 291–301, 2005.](#)

[Mård, J., Box, J. E., Brown, R., Mack, M., Mernild, S. H., Walker, D., Walsh, J., Bhatt, U. S., Epstein, H. E., Myers-Smith, I. H., Reynolds, M. K., and Schuur, E. A. G.: Cross cutting scientific issues, in: Snow, Water, Ice and Permafrost in the Arctic \(SWIPA\) 2017, Arctic Monitoring and Assessment Programme \(AMAP\), Oslo, Norway, 231–256, 2017.](#)

- 25 Marushchak, M. E., Kiepe, I., Biasi, C., Elsakov, V., Friborg, T., Johansson, T., Soegaard, H., Virtanen, T., and Martikainen, P. J.: Carbon dioxide balance of subarctic tundra from plot to regional scales, Biogeosciences, 10, 437–452, 2013.

Marushchak, M. E., Friborg, T., Biasi, C., Herbst, M., Johansson, T., Kiepe, I., Liimatainen, M., Lind, S. E., Martikainen, P. J., Virtanen, T., Soegaard, H., and Shurpali, N. J.: Methane dynamics in the subarctic tundra: combining stable isotope analyses, plot- and ecosystem-scale flux measurements, Biogeosciences 13, 597–608, 2016.

- 30

Matthes, J. H., Sturtevant, C., Verfaillie, J., Knox, S., and Baldocchi, D.: Parsing the variability in CH₄ flux at spatially heterogeneous wetland: Integrating multiple eddy covariance towers with high-resolution flux footprint analysis, J. Geophys. Res.- Biogeo., 119, 1322–1339, 2014.

McGuire, A. D., Christensen, T. R., Hayes, D., Heroult, A., Euskirchen, E., Kimball, J. S., Koven, C., Lafleur, P., Miller, P. A., Oechel, W., Peylin, P., Williams, M., and Yi, Y.: An assessment of the carbon balance of Arctic tundra: comparison among observations, process models, and atmospheric inversions, *Biogeosciences*, 9, 3185–3204, 2012.

Mikola, J., Virtanen, T., Linkosalmi, M., Vähä, E., Nyman, J., Postanogova, O., Räsänen, A., Kotze, D. J., Laurila, T., Juutinen, S., Kondratyev, V., and Aurela, M.: Spatial variation and linkages of soil and vegetation in the Siberian Arctic tundra – coupling field observations with remote sensing data, *Biogeosciences*, 15, 2781–2801, 2018. ~~Discuss.,~~ <https://doi.org/10.5194/bg-2017-569>, in review, 2018.

Nappo, C. J., Caneill, J. Y., Furman, R. W., Gifford, F. A., Kaimal, J. C., Kramer, M. L., Lockhart, T. J., Pendergast, M. M., Pielke, R. A., Randerson, D., Shreffler, J. H., and Wyngaard, J. C.: The workshop on the representativeness of meteorological observations, June 1981, Boulder, Colo., *B. Am. Meteorol. Soc.*, 63, 761–764, 1982.

Neftel, A., Spirig, C., and Ammann, C.: Application and test of a simple tool for operational footprint evaluations, Environ. Pollut., 152, 644–652, 2008.

Nicolini, G., Castaldi, S., Fratini, G., and Valentini, R.: A literature overview of micrometeorological CH₄ and N₂O flux measurements in terrestrial ecosystems, *Atmos. Environ.*, 81, 311–319, 2013.

Nyman, J.: The composition and phenological development of the vegetation and its impact on carbon fluxes in the Siberian tundra, M.Sc. Thesis, Department of Environmental Sciences, University of Helsinki, Finland, 2015.

~~Nzotungicimpaye, C. M. and Zickfeld, K.: The contribution from methane to the permafrost carbon feedback, Curr. Clim. Change Rep., 3, 58–68, 2017.~~

Olefeldt, D., Turetsky, M. R., Crill, P. M., and McGuire, A. D.: Environmental and physical controls on northern terrestrial methane emissions across permafrost zones, *Glob. Change Biol.*, 19, 589–603, 2013.

Parmentier, F. J. W., van Huissteden, J., van der Molen, M. K., Schaepman-Strup, G., Karsanaev, S. A., Maximov, T. C., and Dolman, A. J.: Spatial and temporal dynamics in eddy covariance observations of methane fluxes at a tundra site in northeastern Siberia, *J. Geophys. Res.*, 116, G03016, 2011.

Pasquill, F. and Smith, F. B.: *Atmospheric Diffusion*, 3rd Ed., Ellis Horwood Ltd., Chichester, UK, 1983.

Petrescu, A. M. R., Lohila, A., Tuovinen, J.-P., Baldocchi, D. D., Desai, A. R., Roulet, N. T., Vesala, T., Dolman, A. J., Oechel, W. C., Marcolla, B., Friborg, T., Rinne, J., Matthes, J. H., Merbold, L., Meijide, A., Kiely, G., Sottocornola, M., Sachs, T., Zona, D., Varlagin, A., Lai, D. Y. F., Veenendaal, E., Parmentier, F.-J. W., Skiba, U., Lund, M., Hensen, A., van

- Huissteden, J., Flanagan, L. B., Shurpali, N. J., Grünwald, T., Humphreys, E. R., Jackowicz-Korczyński, M., Aurela, M. A., Laurila, T., Grüning, C., Corradi, C. A. R., Schrier-Uijl, A. P., Christensen, T. R., Tamstorf, M. P., Mastepanov, M., Martikainen, P. J., Verma, S. B., Bernhofer, C., and Cescatti, A.: The uncertain climate footprint of wetlands under human pressure, *P. Natl. Acad. Sci. USA*, 112, 4594–4599, 2015.
- 5 Rebmann, C., Göckede, M., Foken, T., Aubinet, M., Aurela, M., Berbigier, P., Bernhofer, C., Buchmann, N., Carrara, A., Cescatti, A., Ceulemans, R., Clement, R., Elbers, J. A., Granier, A., Grünwald, T., Guyon, D., Havránková, K., Heinesch, B., Knohl, A., Laurila, T., Longdoz, B., Marcolla, B., Markkanen, T., Miglietta, F., Moncrieff, J., Montagnani, L., Moors, E., Nardino, M., Ourcival, J.-M., Rambal, S., Rannik, Ü, Rotenberg, E., Sedlak, P., Unterhuber, G., Vesala, T., and Yakir, D.: Quality analysis applied on eddy covariance measurements at complex sites using footprint modelling, *Theor. Appl.*
- 10 *Climatol.*, 80, 121–141, 2005.
- Riutta, T., Laine, J., Aurela, M., Rinne, J., Vesala, T., Laurila, T., Haapanala, S., Pihlatie, M., and Tuittila, E.-S.: Spatial variation in plant community functions regulates carbon gas dynamics in a boreal fen ecosystem, *Tellus, B* 59, 838–852, 2007.
- Sachs, T., Wille, C., Boike, J., and Kutzbach, L.: Environmental controls on ecosystem-scale CH₄ emission from polygonal
- 15 tundra in the Lena River Delta, Siberia, *J. Geophys. Res.*, 113, G00A03, 2008.
- Sachs, T., Giebels, M., Boike, J., and Kutzbach, L.: Environmental controls on CH₄ emission from polygonal tundra on the microsite scale in the Lena river delta, Siberia, *Glob. Change Biol.*, 16, 3096–3110, 2010.
- Saunois, M., Jackson, R. B., Bousquet, P., Poulter, B., and Canadell, J. G.: The growing role of methane in anthropogenic climate change, *Environ. Res. Lett.*, 11, 120207, 2016.
- 20 ~~Schmid, H. P.: Source area for scalars and scalar fluxes, *Bound. Lay. Meteorol.*, 67, 293–318, 1994.~~
- Schmid, H. P.: Footprint modeling for vegetation atmosphere exchange studies: a review and perspective, *Agr. Forest Meteorol.*, 113, 159–183, 2002.
- Schmid, H. P. and Lloyd, C. R.: Spatial representativeness and the location bias of flux footprints over inhomogeneous areas, *Agr. Forest Meteorol.*, 93, 195–209, 1999.
- 25 Schuur, E. A. G., McGuire, A. D., Schädel, C., Grosse, G., Harden, J. W., Hayes, D. J., Hugelius, G., Koven, C. D., Kuhry, P., Lawrence, D. M., Natali, S. M., Olefeldt, D., Romanovsky, V. E., Schaefer, K., Turetsky, M. R., Treat, C. C., and Vonk, J. E.: Climate change and the permafrost carbon feedback, *Nature*, 520, 171–179, 2015.
- ~~Schneider, J., Grosse, G., and Wagner, D.: Land cover classification of tundra environments in the Arctic Lena Delta based on Landsat 7 ETM+ data and its application for upscaling of methane emissions, *Remote Sens. Environ.*, 113, 380–391, 2009.~~
- 30 ~~2009.~~

- Stow, D. A., Hope, A., McGuire, D., Verbyla, D., Gamon, J., Huemmrich, F., Houston, S., Racine, C., Sturm, M., Tape, K., Hinzman, L., Yoshikawa, K., Tweedie, C., Noyle, B., Silapaswan, C., Douglas, D., Griffith, B., Jia, G., Epstein, H., Walker, D., Daeschner, S., Petersen, A., Zhou, L., and Myneni, R.: Remote sensing of vegetation and land-cover change in Arctic Tundra Ecosystems, *Remote Sens. Environ.*, 89, 281–308, 2004.
- 5 Stoy, P. C., Williams, M., Evans, J. G., Prieto-Blanco, A., Disney, M., Hill, T. C., Ward, H. C., Wade, T. J., and Street, L. E.: Upscaling tundra CO₂ exchange from chamber to eddy covariance tower, *Arct. Antarct. Alp. Res.*, 45, 275–284, 2013.
- [Street, L. E., Shaver, G. R., Williams, M., and Van Wijk, M. T.: What is relationship between changes in canopy leaf area and changes in photosynthetic CO₂ flux in arctic ecosystems?. *J. Ecol.*, 95, 139–150, 2007.](#)
- Tagesson, T., Mölder, M., Mastepanov, M., Sigsgaard, C., Tamstorf, M. P., Lund, M., Falk, J. M., Lindroth, A., Christensen, T. R., and Ström, L.: Land-atmosphere exchange of methane from soil thawing to soil freezing in a high-Arctic wet tundra ecosystem, *Glob. Change Biol.*, 18, 1928–1940, 2012.
- 10 Treat, C. C., Natali, S. M., Ernakovich, J., Iversen, C. M., Lupascu, M., McGuire, A. D., Norby, R. J., Chowdhury, T. R., Richter, A., Šantrůčková, H., Schädel, C., Schuur, E. A. G., Sloan, V. L., Turetsky, M. R., and Waldrop, M. P.: A pan-Arctic synthesis of CH₄ and CO₂ production from anoxic soil incubations, *Glob. Change Biol.*, 21, 2787–2803, 2015.
- 15 [Treat, C. C., Marushchak, M. E., Voigt, C., Zhang, Y., Tan, Z., Zhuang, Q., Virtanen, T. A., Räsänen, A., Biasi, C., Hugelius, G., Kaverin, D., Miller, P. A., Stendel, M., Romanovsky, V., Rivkin, F., Martikainen, P. J., and Shurpali, N. J.: Tundra landscape heterogeneity, not inter-annual variability, controls the decadal regional carbon balance in the Western Russian Arctic, *Glob. Change Biol.*, doi:10.1111/gcb.14421, in press, 2018.](#)
- Tuovinen, J.-P., Aurela, M., and Laurila, T.: Resistances to ozone deposition to a flark fen in the northern aapa mire zone, *J. Geophys. Res.*, 103, 16953–16966, 1998.
- 20 Turetsky, M. R., Kotowska, A., Bubier, J., Dise, N. B., Crill, P., Hornibrook, E. R. C., Minkinen, K., Moore, T. R., Myers-Smith, I. H., Nykänen, H., Olefeldt, D., Rinne, J., Saarnio, S., Shurpali, N., Tuittila, E.-S., Waddington, J. M., White, J. R., Wickland, K. P., and Wilkening, M.: A synthesis of methane emissions from 71 northern, temperate, and subtropical wetlands, *Glob. Change Biol.*, 20, 2183–2197, 2014.
- 25 Turner, M. G. and Chapin III, F. S.: Causes and consequences of spatial heterogeneity in ecosystem function, in: *Ecosystem Function in Heterogeneous Landscapes*, ed: Lovett, G. M., Jones, C. G., Turner, M. G., and Weathers, K. C., Springer Science+Business Media, Inc., New York, 9–30, 2006.
- Uttal, T., Starkweather, S., Drummond, J. R., Vihma, T., Makshtas, A. P., Darby, L. S., Burkhart, J. F., Cox, C. J., Schmeisser, L. N., Haiden, T., Maturilli, M., Shupe, M. D., de Boer, G., Saha, A., Grachev, A. A., Crepinsek, S. M., 30 Bruhwiler, L., Goodison, B., McArthur, B., Walden, V. P., Dlugokencky, E. J., Persson, P. O. G., Lesins, G., Laurila, T., Ogren, J. A., Stone, R., Long, C. N., Sharma, S., Massling, A., Turner, D. D., Stanitski, D. M., Asmi, E., Aurela, M., Skov,

- H., Eleftheriadis, K., Virkkula, A., Platt, A., Førland, E. J., Iijima, Y., Nielsen, I. E., Bergin, M. H., Candlish, L., Zimov, N. S., Zimov, S. A., O'Neill, N. T., Fogal, P. F., Kivi, R., Konopleva-Akish, E. A., Verlinde, J., Kustov, V. Y., Vassel, B., Ivakhov, V. M., Viisanen, Y., and Intrieri, J. M.: International Arctic Systems for Observing the Atmosphere (IASOA): An International Polar Year Legacy Consortium, *B. Am. Meteorol. Soc.*, 97, 1034–1056, 2016.
- 5 Vähä, E.: Kasvillisuus- ja maaperämuuttujien välinen yhteys ja niiden merkitys hiilidioksidin ja metaanin vaihdossa arktisen tundraekosysteemin ja ilmakehän välillä [The relationship between vegetation and soil variables and their importance in the carbon dioxide and methane exchange between an Arctic tundra ecosystem and the atmosphere], M.Sc. Thesis, Department of Environmental Sciences, University of Helsinki, Finland, 2016.
- Virkkala, A.-M., Virtanen, T., Lehtonen, A., Rinne, J., and Luoto, M.: The current state of CO₂ flux chamber studies in the Arctic tundra: a review, *Prog. Phys. Geog.*, [42, 162–184, 2017, DOI:10.1177/0309133317745784, 2017.](#)
- 10 | Virtanen, T. and Ek, M.: The fragmented nature of tundra landscape, *Int. J. Appl. Earth Obs.*, 27, 4–12, 2014.
- Wang, H., Jia, G., Zhang, A., and Miao, C.: Assessment of spatial representativeness of eddy covariance flux data from flux tower to regional grid, *Remote Sens.*, 8, 742, 2016.
- Whalen, S. C. and Reeburgh, W. S.: Consumption of atmospheric methane by tundra soils, *Nature*, 346, 160–162, 1990.
- 15 Wik, M., Varner, R. K., Walter Anthony, K., MacIntyre, S., and Bastviken, D.: Climate-sensitive northern lakes and ponds are critical components of methane release, *Nat. Geosci.*, 9, 99–106, 2016.
- [Wille, C., Kutzbach, L., Sachs, T., Wagner, D., and Pfeiffer, E.-M.: Methane emission from Siperian arctic polygonal tundra: eddy covariance measurements and modeling, *Glob. Change Biol.*, 14, 1395–1408, 2008.](#)
- 20 Yu, L., Wang, H., Wang, G., Song, W., Huang, Y., Li, S.-G., Liang, Y., Tang, Y., and He, J.-S.: A comparison of methane emission measurements using eddy covariance and manual and automated chamber-based techniques in Tibetan Plateau alpine wetland, *Environ. Pollut.*, 181, 81–90, 2013.
- [Zona, D., Oechel, W. C., Kochendorfer, J., Paw U, K. T., Salyuk, A. N., Olivas, P. C., Oberbauer, S. F., and Lipson, D. A.: Methane fluxes during the initiation of a large-scale water table manipulation experiment in the Alaskan Arctic tundra, *Global Biogeochem. Cy.*, 23, GB2013, 2009.](#)

|

Table 1. Land cover classes and their dominating vegetation and other characteristics, derived from Juutinen et al. (2017) and Mikola et al. (2018).

<u>Class</u>	<u>Peat layer</u>	<u>Mosses and lichens</u>	<u>Vascular plants</u>	<u>Other</u>
<u>Wet fen</u>	<u>yes</u>	<u>sparse wet brown moss cover</u>	<u>sedge-dominated</u>	<u>high water table, water pools</u>
<u>Dry fen</u>	<u>yes</u>	<u>dense <i>Sphagnum</i> cover, some wet brown mosses</u>	<u>some sedges and dwarf shrubs</u>	<u>water table below moss layer</u>
<u>Bog</u>	<u>yes</u>	<u><i>Sphagnum</i>-dominated</u>	<u>dwarf shrubs, <i>Betula nana</i></u>	<u>hummock-hollow surface pattern</u>
<u>Graminoid tundra</u>	<u>no</u>	<u>some feather mosses</u>	<u>graminoid-dominated; other vascular plants may occur</u>	
<u>Flood meadow</u>	<u>no</u>	<u>some wet brown mosses, no <i>Sphagnum</i></u>	<u>graminoid-dominated; herbs, willows</u>	<u>brookside spring flooding area</u>
<u>Shrub tundra</u>	<u>no</u>	<u>feather moss cover, no <i>Sphagnum</i>; some lichens</u>	<u>dwarf shrubs, <i>Betula nana</i></u>	
<u>Lichen tundra</u>	<u>no</u>	<u>lichen-dominated; some feather mosses</u>	<u>some herbs and dwarf shrubs</u>	<u>alternates with bare ground</u>
<u>Bare ground</u>	<u>no</u>			<u>non-vegetated</u>
<u>Water</u>	<u>no</u>			<u>sea, freshwater bodies</u>

Table 24. Flow conditions assumed for the example calculations.

Case	L^{-1} (m ⁻¹)	u_* (m s ⁻¹)	σ_v (m s ⁻¹)	U (m s ⁻¹)
Unstable	-0.2	0.15	0.35	1.8
Neutral	0	0.40	0.92	5.7
Stable	0.1	0.10	0.23	1.8

5 |

Table 32. Aggregated land cover classes for the regression model.

LCC group description	LCCs included
Strong source	Wet fen, TWI > 4 Graminoid tundra, TWI > 4
Moderate source	Wet fen, TWI ≤ 4 Dry fen Water, above sea level
Sink	Bare ground Lichen tundra
Neutral	Other

Table 3. Source area dimensions for the example cases specified in Table 1, calculated according to different definitions: (1) Single three dimensional footprint Π , Eq. (3); (2) Single cross wind integrated footprint Π_C , Eq. (7); and (3) Annular footprint climatology Π^* , Eq. (4).

Case ^a	$P = 25\%$	$P = 50\%$	$P = 75\%$	$P = 90\%$	
(1) Single three dimensional (Π)					
	r_{\max} (m)	$r_{P,1} - r_{P,2}$ [max. width] ^b (m)			
Unstable	18	10–37 [12]	8–59 [21]	6–107 [40]	5–206 [74]
Neutral	27	13–75 [22]	9–143 [45]	7–338 [102]	5–915 [247]
Stable	35	15–126 [33]	10–287 [76]	7–897 [206]	5–3545 [652]
(2) Single cross wind integrated (Π_C)					
	r_{\max} (m)	x_P (m)			
Unstable	23	27	46	86	168
Neutral	39	56	112	269	734
Stable	53	94	223	706	2805
(3) Annular climatology (Π^*)					
	r_{\max} (m)	$r_{P,1} - r_{P,2}$ (m)			
Unstable	18	11–29	8–47	6–87	5–170
Neutral	26	14–57	10–113	7–272	5–740
Stable	34	16–95	11–225	7–711	5–2816

^aSymbols: P = proportion of the measured flux originating from the surface elements within the dimensions indicated; r_{\max} = distance of the footprint maximum; $r_{P,1}, r_{P,2}$ = distances between which the surface elements with the largest contribution to P are located; x_P = distance integrated from the EC tower location within which P originates from.

^bMaximum width of the source area.

5

Table 4. Proportions (%) of different land cover classes as weighted by the mean footprint function during the growing season (“Weighted”) and their areal coverages within the study area (“Area”), within the source area defined by the 90 % cumulative footprint (“Area, 90 %”; Eq. 3, $P = 90\%$), within a distance of 1 km from the EC tower (“Area, 1 km”) and within a 35.8 km² region (“Region”, Fig. S1 in the Supplement). The values in parentheses indicate the proportions if the water pixels representing marine areas are removed and the integrated footprint within the study area is scaled to 100 %.

Land cover class	—Weighted		—Area		—Area, 90 %		—Area, 1 km		—Region	
Wet fen	8.5	(11.9)	15.1	(17.7)	15.0	(15.1)	17.9	(19.7)	15.6	(16.4)
Dry fen	16.2	(17.5)	10.9	(12.8)	10.3	(10.3)	10.4	(11.4)	11.1	(11.6)
Bog	16.9	(17.7)	10.9	(12.8)	22.9	(23.0)	13.0	(14.3)	8.7	(9.1)
Graminoid tundra	11.1	(15.1)	5.6	(6.6)	11.5	(11.6)	6.9	(7.6)	3.2	(3.4)
Flood meadow	3.1	(4.0)	0.6	(0.7)	1.4	(1.4)	0.8	(0.9)	0.4	(0.4)
Shrub tundra	12.2	(11.5)	17.9	(21.1)	18.2	(18.2)	17.8	(19.6)	26.2	(27.4)
Lichen tundra	14.3	(12.1)	10.5	(12.4)	10.9	(10.9)	9.9	(10.9)	10.7	(11.1)
Bare ground	12.4	(9.9)	11.6	(13.6)	8.0	(8.0)	12.8	(14.1)	14.6	(15.3)
Water	1.0	(0.3)	16.9	(2.3)	1.9	(1.4)	10.6	(1.6)	9.4	(5.3)
Out [†]	4.3	(0.0)	—	—	—	—	—	—	—	—
Total	100.0	(100.0)	100.0	(100.0)	100.0	(100.0)	100.0	(100.0)	100.0	(100.0)

[†]Cumulative proportion of the footprint exceeding the limits of the study area

10

Table 4. Proportions (%) of different land cover classes as weighted by the mean footprint function during the growing season (“Weighted”) and their areal coverages within the study area (“Area”), within the source area defined by the 90 % cumulative footprint (“Area, 90 %”, Fig. 1a), and within a 35.8 km² region (“Region”, Fig. S2 in the Supplement). The marine areas are excluded, and the integrated footprint within the study area is scaled to 100 %.

Land cover class	Weighted	Area	Area, 90 %	Region
Wet fen	<u>9.0</u>	<u>17.7</u>	<u>15.1</u>	<u>16.4</u>
Dry fen	<u>17.0</u>	<u>12.8</u>	<u>10.3</u>	<u>11.6</u>
Bog	<u>17.8</u>	<u>12.8</u>	<u>23.0</u>	<u>9.1</u>
Graminoid tundra	<u>11.7</u>	<u>6.6</u>	<u>11.6</u>	<u>3.4</u>
Flood meadow	<u>3.3</u>	<u>0.7</u>	<u>1.4</u>	<u>0.4</u>
Shrub tundra	<u>12.8</u>	<u>21.1</u>	<u>18.2</u>	<u>27.4</u>
Lichen tundra	<u>15.1</u>	<u>12.4</u>	<u>10.9</u>	<u>11.1</u>
Bare ground	<u>13.0</u>	<u>13.6</u>	<u>8.0</u>	<u>15.3</u>

<u>Water</u>	<u>0.2</u>	<u>2.3</u>	<u>1.4</u>	<u>5.3</u>
<u>Total</u>	<u>100.0</u>	<u>100.0</u>	<u>100.0</u>	<u>100.0</u>

Table 5. Estimated CH_4 fluxes for the aggregated land cover classes.

LCC group description	CH_4 flux ($\mu\text{g CH}_4 \text{ m}^{-2} \text{ s}^{-1}$)	95 % confidence interval ($\mu\text{g CH}_4 \text{ m}^{-2} \text{ s}^{-1}$)
Strong source	0.949	[0.871, 1.028]
Moderate source	0.264	[0.180, 0.348]
Sink	-0.131	[-0.172, -0.089]
Neutral	-0.007	[-0.035, 0.021]

5

Table 6. Upscaling of CH₄ fluxes ($\mu\text{g CH}_4 \text{ m}^{-2} \text{ s}^{-1}$) ~~for different areas~~ based on the LCC group-specific flux data shown in Table 5.

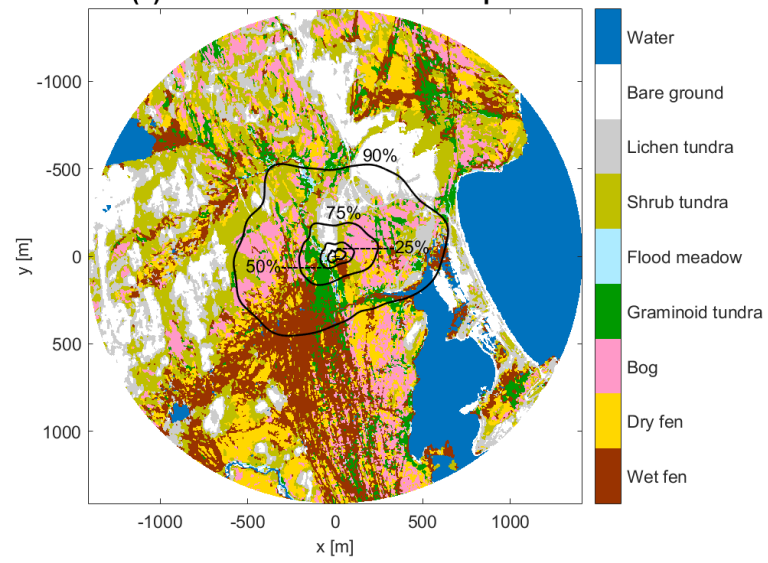
5

<u>LCC group</u>	<u>Study area^a</u> <u>(6.3 km²)</u>		<u>Region^a</u> <u>(35.8 km²)</u>	
	<u>Coverage^b (%)</u>	<u>Flux^c</u>	<u>Coverage (%)</u>	<u>Flux</u>
<u>Strong source</u>	<u>17.7</u>	<u>0.168</u> <u>(91.8 %)</u>	<u>15.1</u>	<u>0.144</u> <u>(89.8 %)</u>
<u>Moderate source</u>	<u>19.5</u>	<u>0.052</u> <u>(28.3 %)</u>	<u>20.3</u>	<u>0.054</u> <u>(33.5 %)</u>
<u>Sink</u>	<u>26.0</u>	<u>-0.034</u> <u>(-18.6 %)</u>	<u>26.4</u>	<u>-0.035</u> <u>(-21.6 %)</u>
<u>Neutral</u>	<u>36.8</u>	<u>-0.003</u> <u>(-1.4 %)</u>	<u>38.1</u>	<u>-0.003</u> <u>(-1.7 %)</u>
<u>Upscaled flux^d</u>		<u>0.183</u> <u>[0.156, 0.209]</u>		<u>0.160</u> <u>[0.134, 0.186]</u>

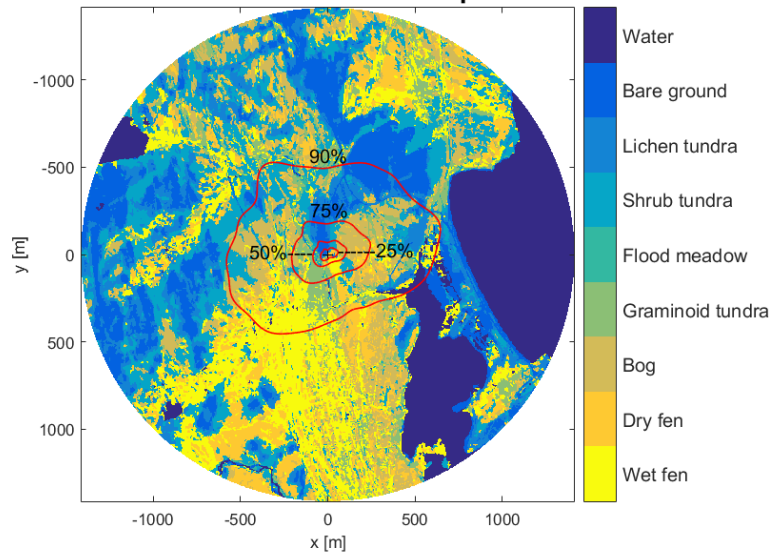
^a “Study area” refers to the circle with a radius of 1.4 km centred at the EC mast; “Region” is shown in Fig. S2 (in the Supplement).

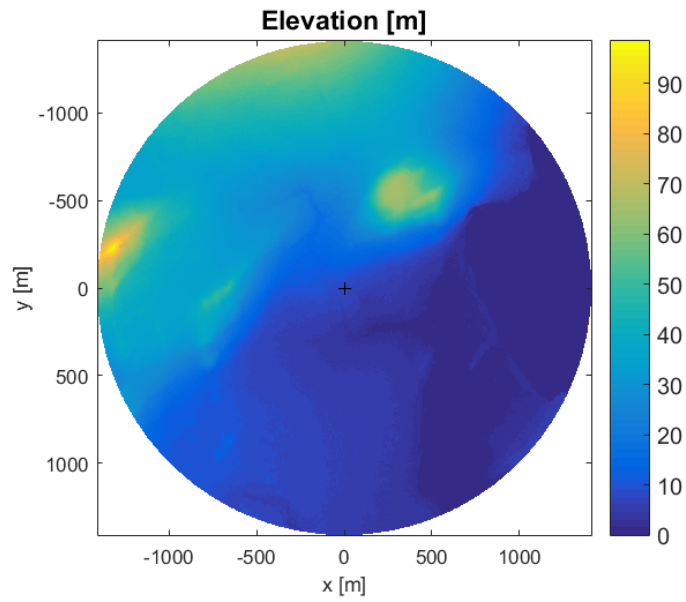
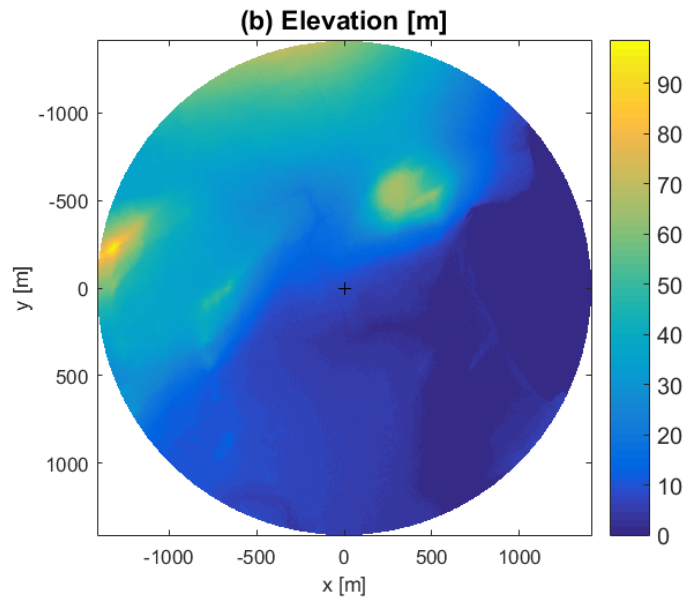
^b Marine areas are excluded from upscaling. ^c Calculated as LCC group-specific flux \times relative coverage. The value in parentheses equals this flux divided by the upscaled flux. ^d The values in square brackets indicate the 95 % confidence interval.

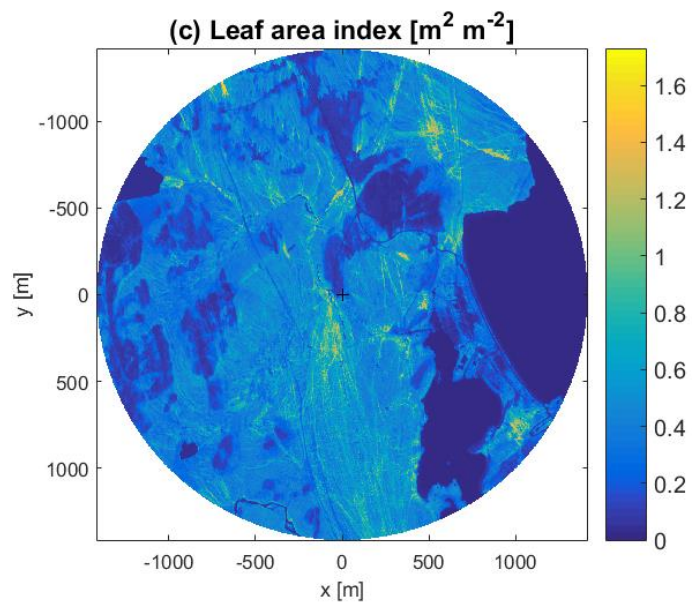
(a) Land cover and mean footprint

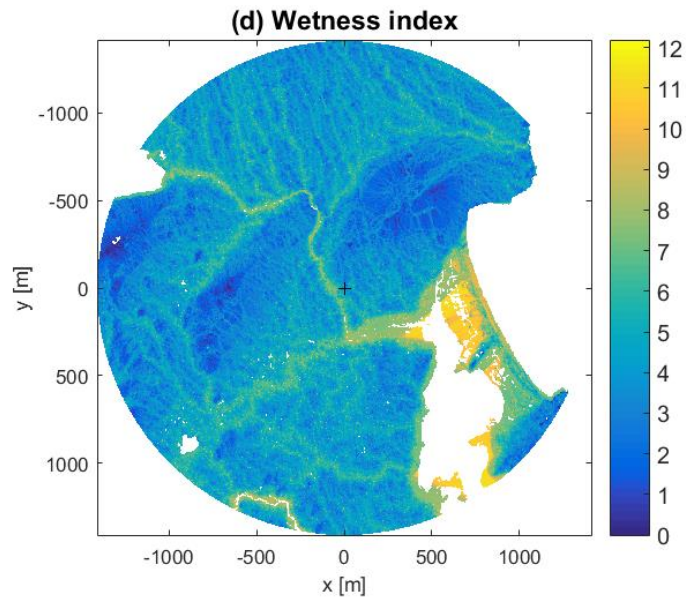
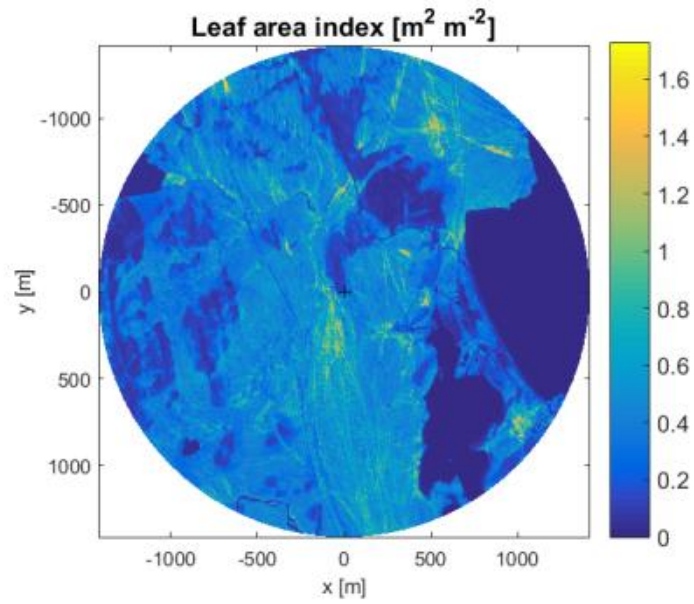


Land cover and mean footprint









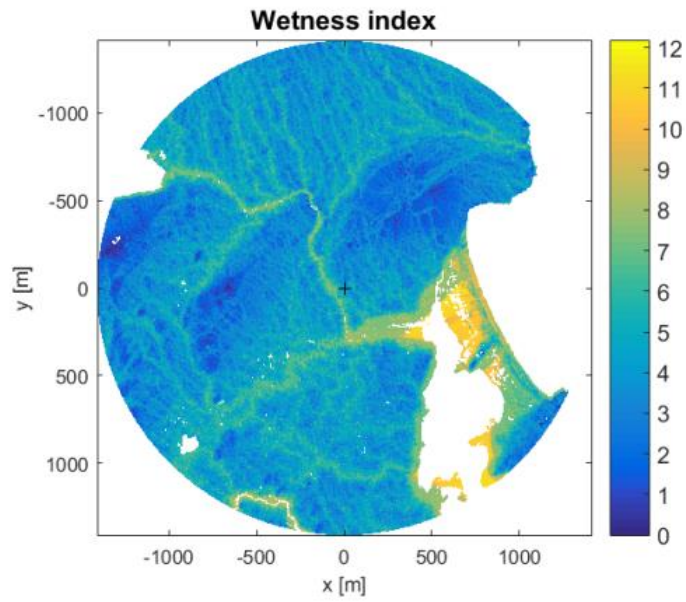
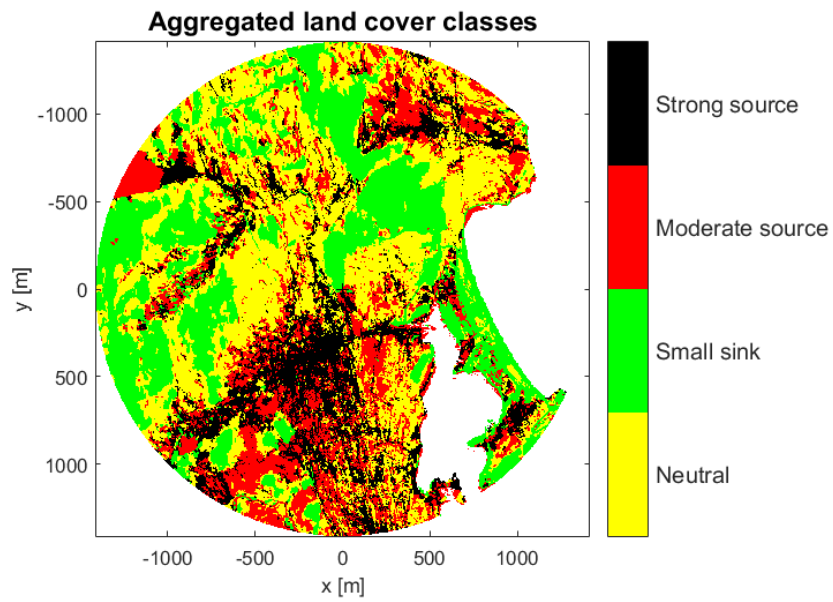
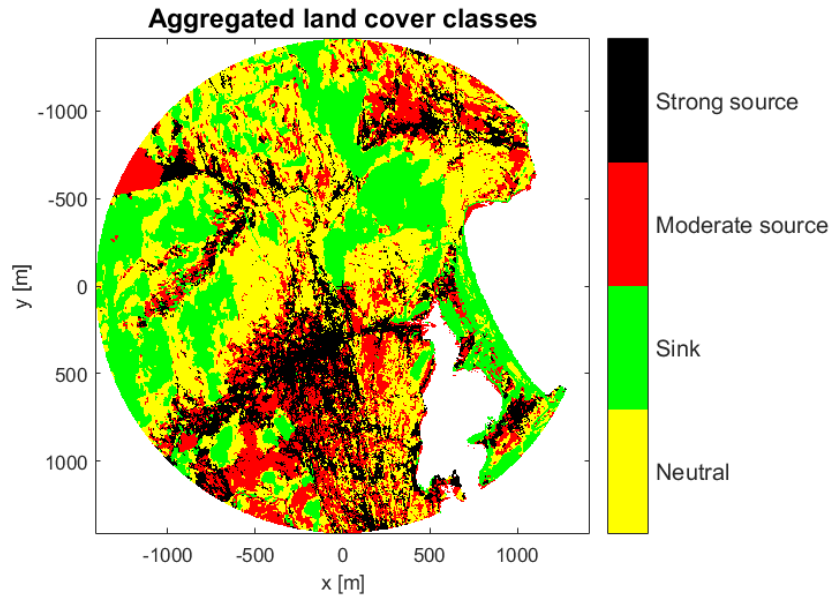
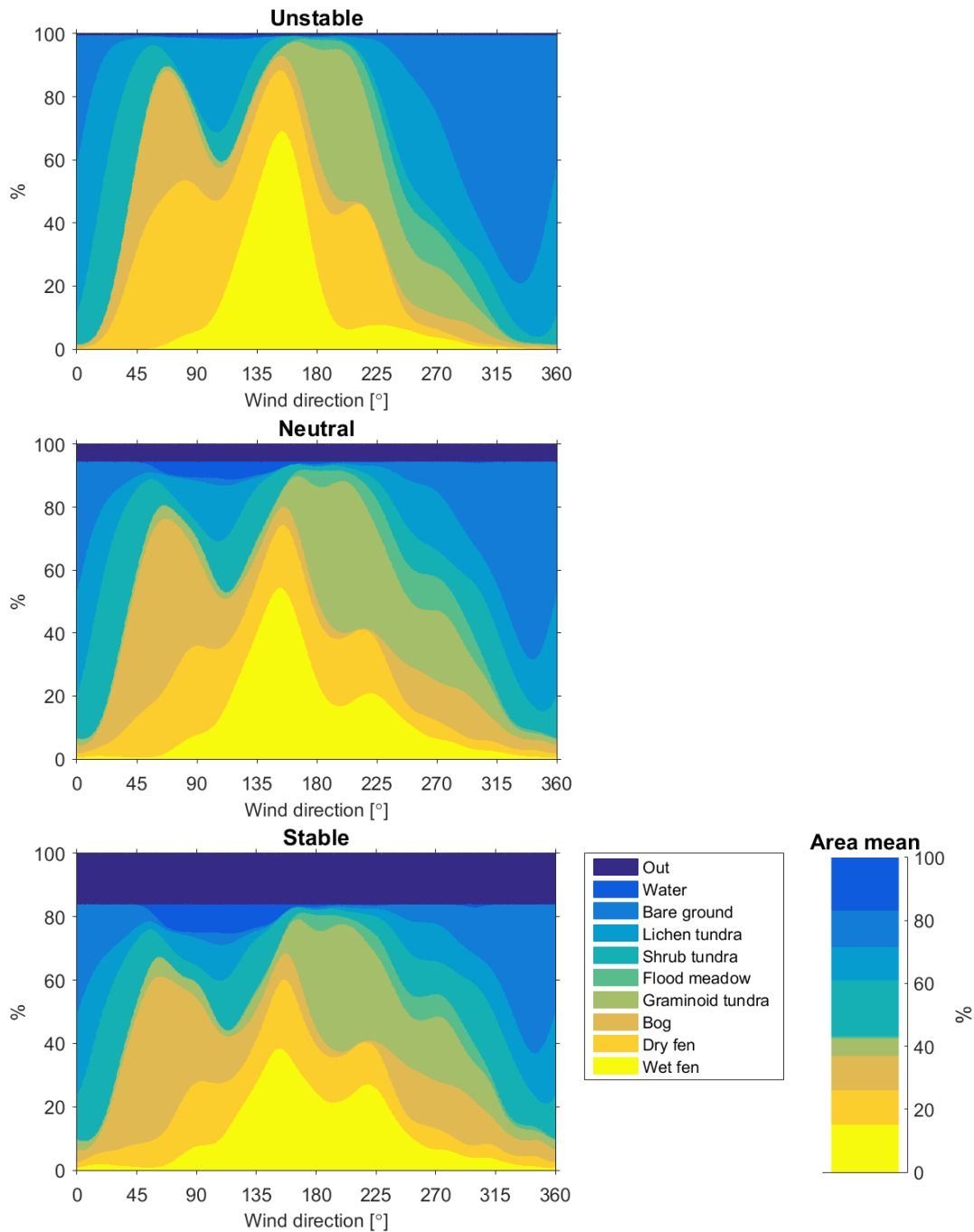


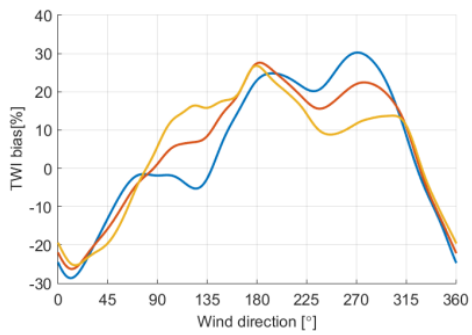
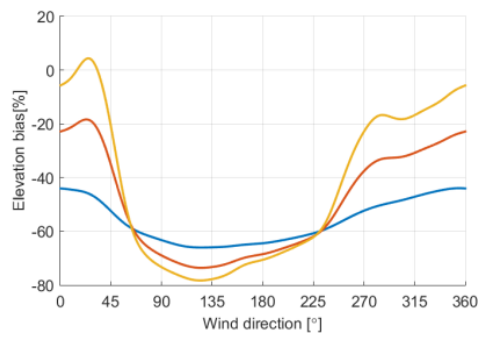
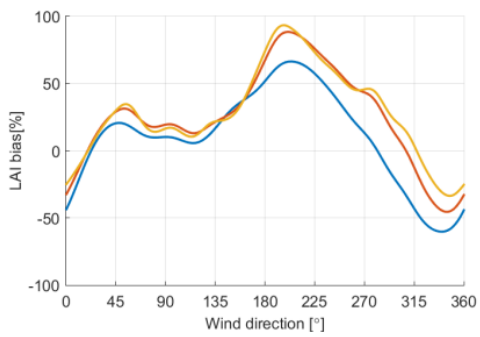
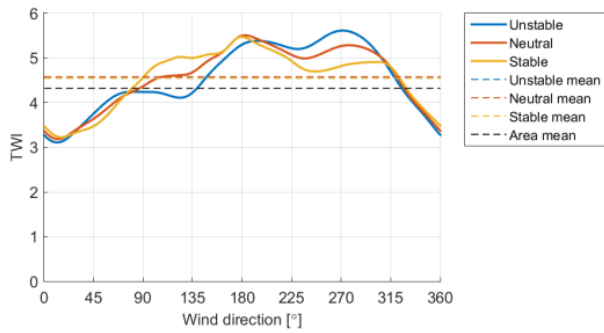
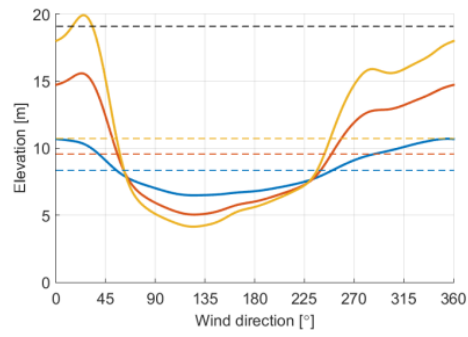
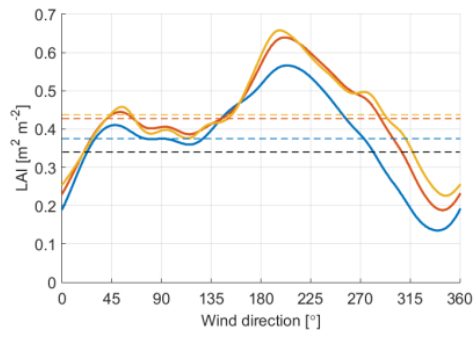
Figure 1. Land cover classes and the mean cumulative footprint during the growing season of 2014 (a), maximum leaf area index (on 12 August 2012) (b), terrain elevation (c) and topographic wetness index for terrestrial surfaces (d). The isophlets in (a) indicate the areas with a 25, 50, 75 and 90 % contribution to the measured flux only the further distance visible. The plus sign indicates the location of the EC tower.



5 Figure 2. Distribution of the aggregated land cover classes (excluding marine areas).



5 Figure 3. Proportion of different land cover classes in the flux footprint as a function of wind direction for the three flow condition cases specified in Table 42. The rightmost panel shows the relative coverage of these classes within the study area (%).



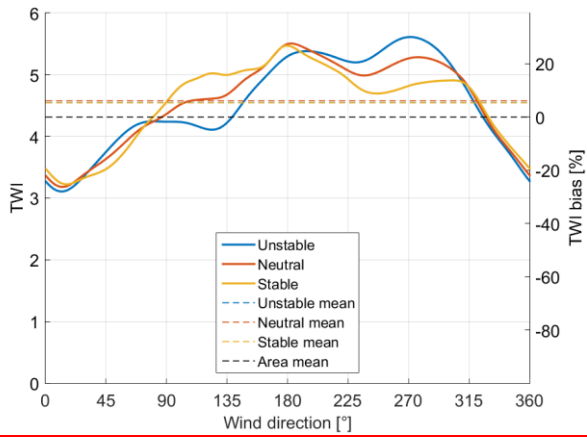
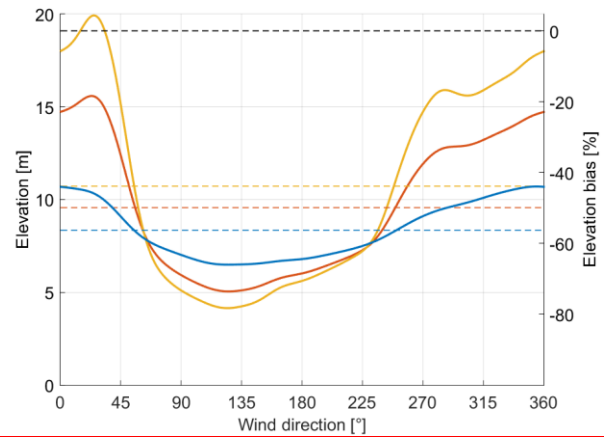
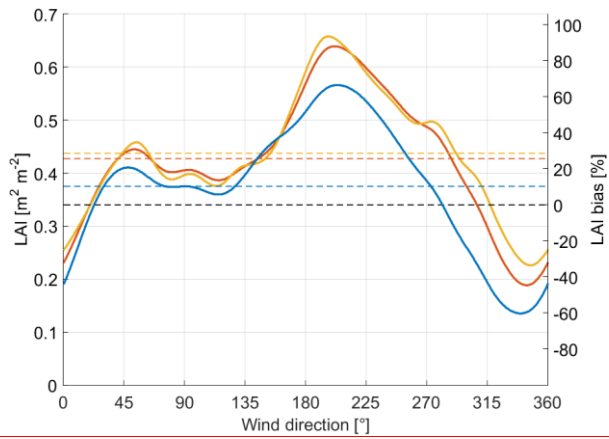


Figure 4. The footprint-weighted and areally averaged leaf area index (a), terrain elevation (b) and topographic wetness index (c), ~~and the corresponding sensor location biases (d-f)~~ as a function of wind direction for the three flow condition cases specified in Table 42. The right-hand ordinate indicates the corresponding sensor location bias.

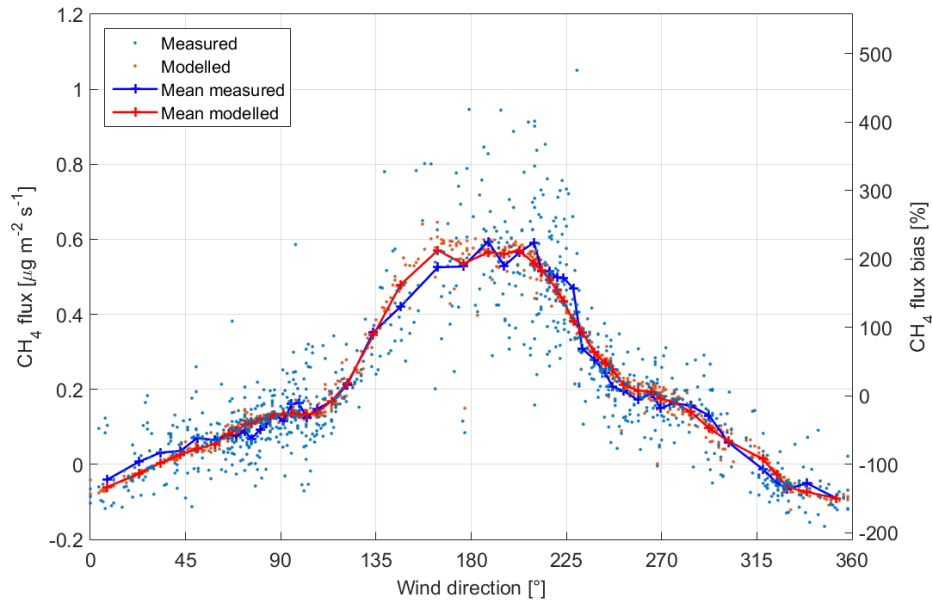
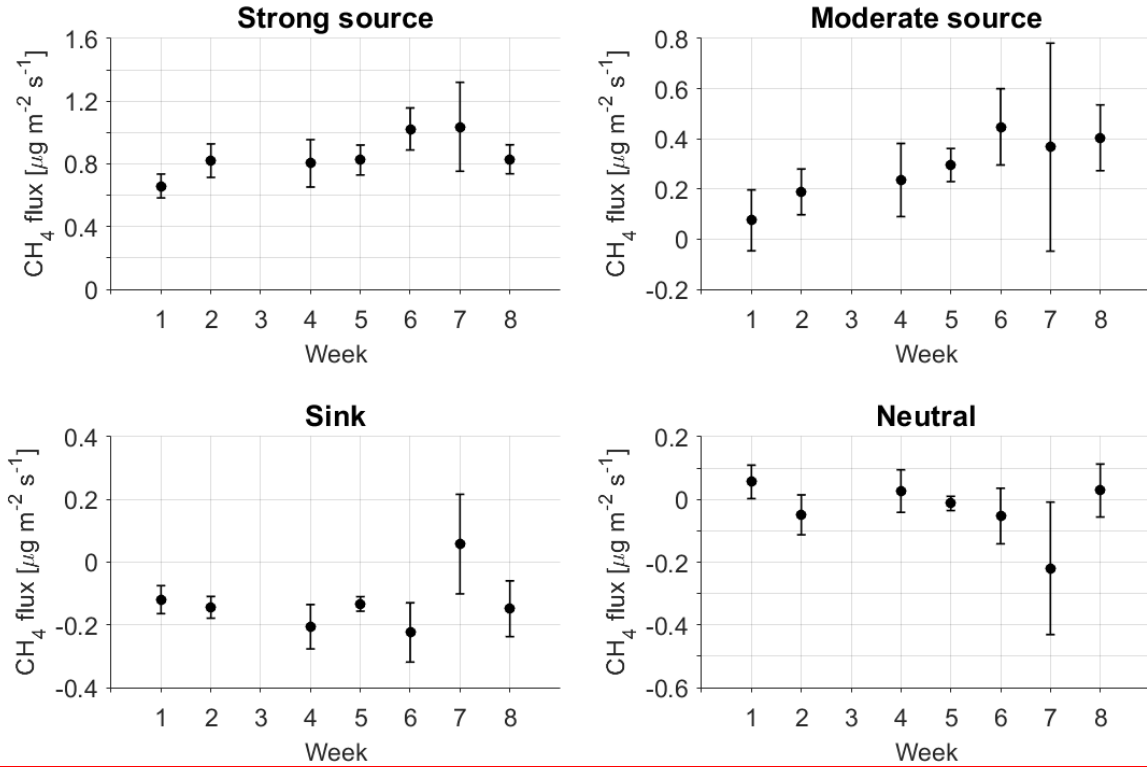
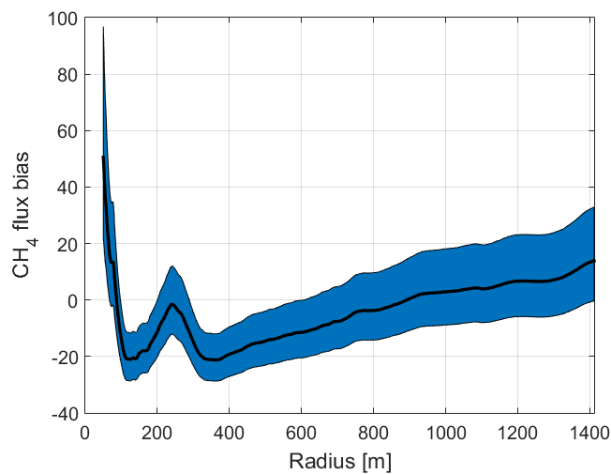
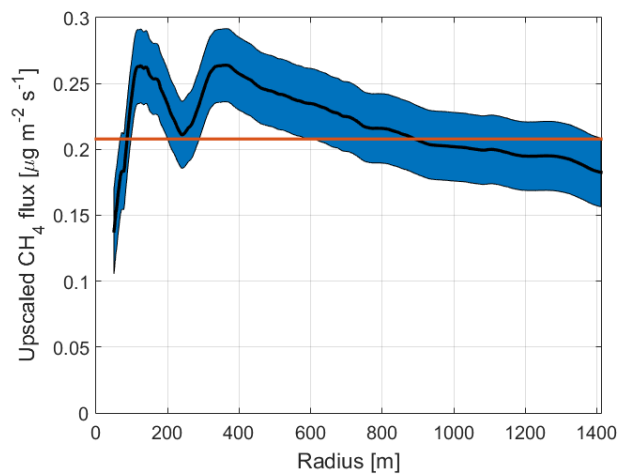
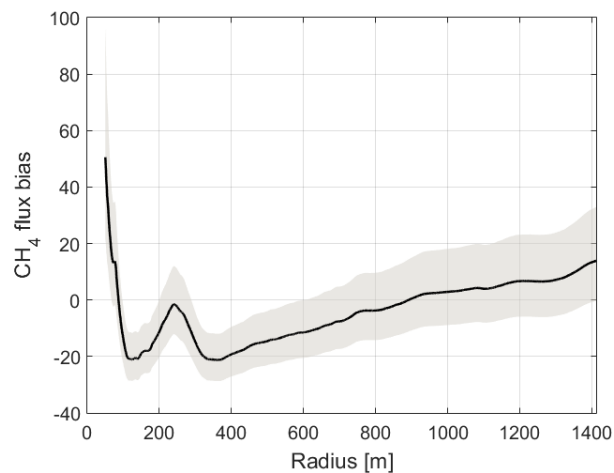
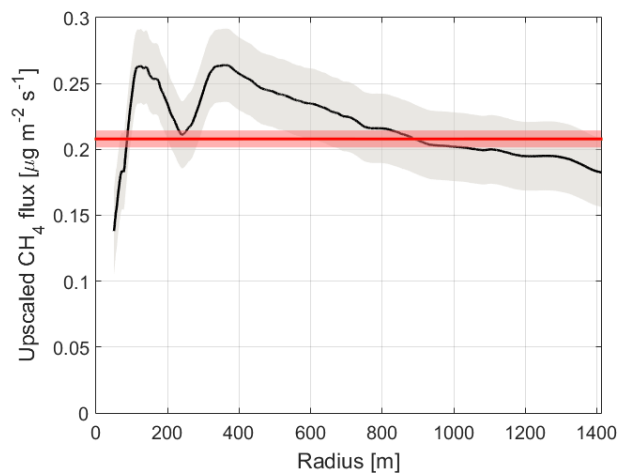


Figure 5. Measured and modelled CH_4 fluxes as a function of wind direction (left axis). The averaged data were calculated in 50 direction classes. The right axis indicates the sensor location bias of the measured data shown (both individual points and the mean) with respect to the mean upscaled flux within the study area ($0.183 \mu\text{g CH}_4 \text{ m}^{-2} \text{ s}^{-1}$).



5 Figure 6. Estimates of the LCC group-specific fluxes calculated from weekly data (1 = 5–11 July; 2 = 12–18 July; 3 = 19–25 July, data missing; 4 = 26 July –1 August; 5 = 2–8 August; 6 = 9–15 August; 7 = 16–22 August; 8 = 23–29 August). The vertical bars indicate the 95 % confidence intervals.



5 Figure 76. Upscaled CH₄ flux within a circular area as a function of the distance from the EC tower (left), and the corresponding sensor location bias according to Eq. (54) (right). The red line indicates the mean measured flux. The shaded areas represents the 95 % confidence intervals determined from the data shown in Table 5.